



UNIVERSITY OF LEEDS

This is a repository copy of *Internal forces of underground structures from observed displacements*.

White Rose Research Online URL for this paper:
<http://eprints.whiterose.ac.uk/84033/>

Version: Accepted Version

Article:

Fuentes, R (2015) Internal forces of underground structures from observed displacements. *Tunnelling and Underground Space Technology*, 49. pp. 50-66. ISSN 0886-7798

<https://doi.org/10.1016/j.tust.2015.03.002>

© 2015, Elsevier Ltd. Licensed under the Creative Commons Attribution-NonCommercial-NoDerivatives 4.0 International
<http://creativecommons.org/licenses/by-nc-nd/4.0/>

Reuse

Unless indicated otherwise, fulltext items are protected by copyright with all rights reserved. The copyright exception in section 29 of the Copyright, Designs and Patents Act 1988 allows the making of a single copy solely for the purpose of non-commercial research or private study within the limits of fair dealing. The publisher or other rights-holder may allow further reproduction and re-use of this version - refer to the White Rose Research Online record for this item. Where records identify the publisher as the copyright holder, users can verify any specific terms of use on the publisher's website.

Takedown

If you consider content in White Rose Research Online to be in breach of UK law, please notify us by emailing eprints@whiterose.ac.uk including the URL of the record and the reason for the withdrawal request.



eprints@whiterose.ac.uk
<https://eprints.whiterose.ac.uk/>

Manuscript Number: TUST-D-14-00285R1

Title: Internal forces of underground structures from observed displacements

Article Type: Research Paper

Section/Category: Tunnelling

Keywords: Axial forces, Curvature, Moment distributions, Piles, Retaining structures, Soil/structure interactions, Tunnels

Corresponding Author: Dr. Raul Fuentes, EngD, MSc, Ingeniero

Corresponding Author's Institution: University of Leeds

First Author: Raul Fuentes, EngD, MSc, Ingeniero

Order of Authors: Raul Fuentes, EngD, MSc, Ingeniero

Abstract: This paper presents a method that provides a solution to the long standing problem of calculating internal force distributions based on displacement measurements of piles, retaining walls and tunnels. It is based on the principle of virtual work and therefore, analytically correct in the linear elastic range, and works without the need of any boundary conditions. The validation against multiple case studies, showcasing loading conditions including seismic, earth pressures, external loads, or sliding slopes in multiple ground conditions and construction processes, confirms its flexibility and applicability to any structure where displacements are observed. Although the validation presented here applies to bending moments and axial forces, the method is theoretically correct and applicable to other internal force distributions.

Highlights

- Analytical solution for the internal forces of piles, retaining walls & tunnels
- Works for any load condition and does not require boundary conditions.
- Calculates both axial forces and bending moments in tunnel linings

Title: Internal forces of underground structures from observed displacements

Author: Raul Fuentes,

EUR ING, MSc, EngD, Ing., Civiling. MIDA, CEng MICE

Address: School of Civil Engineering, University of Leeds, Leeds, LS2 9JT

Telephone: (+44) 0113 343 2282

Email: r.fuentes@leeds.ac.uk

1 **ABSTRACT**

2 This paper presents a method that provides a solution to the long standing problem of
3 calculating internal force distributions based on displacement measurements of piles,
4 retaining walls and tunnels. It is based on the principle of virtual work and therefore,
5 analytically correct in the linear elastic range, and works without the need of any
6 boundary conditions.

7 The validation against multiple case studies, showcasing loading conditions including
8 seismic, earth pressures, external loads, or sliding slopes in multiple ground conditions
9 and construction processes, confirms its flexibility and applicability to any structure
10 where displacements are observed. Although the validation presented here applies to
11 bending moments and axial forces, the method is theoretically correct and applicable to
12 other internal force distributions.

13 **Keywords:** Axial forces, Curvature, Moment distributions, Piles, Retaining structures,
14 Soil/structure interactions, Tunnels.

15 **INTRODUCTION**

16 The behaviour and structural design of underground structures is governed by the
17 distribution of internal forces. Out of these internal forces, bending moments are most
18 critical for structures supporting bending forces, such as laterally loaded piles and
19 retaining walls, and subsequently for the amount of reinforcement that the structure
20 must be provided with. In tunnels, axial forces are equally relevant, not for
21 reinforcement considerations only, but to guarantee its stability as well. However,
22 despite the importance of these internal forces, traditional monitoring techniques of
23 these structures concentrate on measuring total or relative deformations to verify design

24 assumptions rather than enabling direct conclusions about the governing internal forces
25 of the structure itself.

26 This disconnection between monitoring and design parameters arises for two main
27 reasons (Fuentes, 2012): lack of proven and widely accepted monitoring techniques to
28 measure internal forces, especially bending moments, and the lack of a general method
29 to translate displacement measurements into internal forces.

30 With regards to bending moments, and in response to the first of the above
31 shortcomings, some have recently developed techniques using fibre optics that are
32 capable of measuring bending moments or curvature indirectly (e.g. see Inaudi et al,
33 1998; Mohamad et al, 2010, 2011 and 2012; Fuentes, 2012). However, this technique is
34 still suffering from the fact that measurements are indirect – i.e. curvature is inferred
35 from axial strains – and that in order to obtain other relevant parameters, such as
36 displacements, a cumbersome double integration needs to be carried out. Nip & Ng
37 (2005) illustrated the problems of this integration process based on beam theory and
38 overcame this successfully defining multiple boundary conditions over a controlled pile
39 test and applying an iterative process to calculate the integration constants and fitting
40 parameters. However, due to these conditions, the method cannot be simply used for
41 other structures where less control over the boundary conditions is present. Mohamad
42 et al (2011) used a numerical integration and boundary conditions of zero rotation and
43 displacement at the wall toe, which were reasonable due to the depth of the wall under
44 consideration. For less deep structures this assumption would be incorrect and hence
45 further measurements, additional known boundary conditions or both must be provided.

46 Furthermore, it must be noted that calculation of displacements from curvature provides
47 only part of the total displacement as it ignores rigid body translations and rotations.

48 The second shortcoming, translating displacements into bending moments or curvature,
49 has been, to date, challenging. It involves the double derivation of a fitted curve to the
50 displacement profile that, as Brown et al (1994) highlighted, often presents difficulties
51 and errors that propagate through the double derivation process. In order to reduce
52 these errors, multiple readings are needed and other boundary conditions need to be
53 imposed in advance so that the results are acceptable. Hence, although satisfactory
54 solutions have been provided in the literature, these apply to specific conditions and
55 structures and therefore, need to be used with caution elsewhere.

56 The situation in tunnels is even more problematic as the available solutions to obtain
57 bending moments and axial loads from displacements involve back-calculation and
58 iterative processes using models that are successful in forward prediction - e.g.
59 continuum models (Muir Wood, 1975; Curtis, 1976; Einstein & Schwartz, 1979;
60 Duddeck & Erdman, 1985; El Naggar et al, 2008 and Carranza-Torres, 2013),
61 convergence-confinement methods (e.g. Panet and Guenot, 1982), bedded beam
62 springs (ITA, 1998; Oreste, 2003) or finite element analysis. Although satisfactory in its
63 forward use, they also apply to specific conditions and still do not provide an
64 independent check on the original calculation method.

65 This paper presents the first application of the unit-load to the calculation of internal
66 forces - You et al (2007) used its more typical application for displacement calculations
67 for a shield tunnel and, similarly, Kim (1996) used it for validating the displacements
68 obtained from predictive methods in model tunnels. It is based on the principle of virtual

69 work, and enables calculating the internal force distributions of piles, retaining walls and
70 tunnels when the displacements of the structure are known, without the need of any
71 boundary conditions. The validation here concentrates on bending moments for all three
72 structure types and axial forces in tunnels, as they are the most relevant to their
73 performance. However, the methodology would equally apply to other internal force
74 distributions.

75 **THE UNIT-LOAD METHOD IN ITS TRADITIONAL USE**

76 The unit-load (UL) method uses the principle of virtual work and is widely used in
77 structural engineering for the calculation of displacements of structures. Its
78 implementation involves the definition of two structural systems: one comprising the real
79 structure with its external loads (denoted here as ‘real’) and the second (denoted as ‘1’)
80 consisting of the same structure with only a single unit-load applied at the point and in
81 the direction of the displacement to be calculated. Once the two systems are defined,
82 Gere and Timoshenko (1987) show that the displacement, u , of the real structure at the
83 point of application of the unit-load is

$$84 \quad u = \int N_1 d\delta + \int M_1 d\theta + \int V_1 d\rho + \int T_1 d\gamma \quad (1)$$

85 where N_1 , M_1 , V_1 and T_1 are respectively the normal stress, bending moments, shear
86 stress and torsion internal force distributions of the unit-load structure. The second term
87 in each integral represents the corresponding small displacement of the real system.

88 The above equation applies to any material behaviour as long as the displacement
89 terms are small (Gere & Timoshenko, 1987). For a linear elastic material, where the
90 deformations are related to the internal forces through well-known elasticity constants, it
91 becomes

92
$$u = \int \frac{N_1 N_{real}}{EA} dx + \int \frac{M_1 M_{real}}{EI} dx + \int \frac{\alpha_s V_1 V_{real}}{GA} dx + \int \frac{T_1 T_{real}}{GI_p} dx \quad (2)$$

93 where E is the elastic Young's modulus, G the shear modulus, I the second moment of
 94 inertia, A, the area of the cross section and I_p the polar moment of inertia.

95 **PROPOSED METHOD**

96 Reversing equation (2) allows calculation of the internal forces of the real structure,
 97 N_{real} , M_{real} , V_{real} or T_{real} , based on the observed displacements, u , at a given time.

98 If N_{real} , M_{real} , V_{real} or T_{real} adopt a generalised linear equation of the form

99
$$N_{real}, M_{real}, V_{real}, T_{real} = f(x) = C_0 + C_1 f_1(x) + C_2 f_2(x) + \dots + C_n f_n(x) \quad (3)$$

100 the constants C and integrals can be separated and equation (1) can be written in its
 101 matrix form

102
$$\mathbf{u} = \mathbf{B}_N \cdot \mathbf{C}_N + \mathbf{B}_M \cdot \mathbf{C}_M + \mathbf{B}_V \cdot \mathbf{C}_V + \mathbf{B}_T \cdot \mathbf{C}_T \quad (4)$$

103 where the different suffices refer to each of the internal force distributions; \mathbf{u} is the array
 104 containing all of the observed displacements, generally of dimensions (k,1); \mathbf{C} (n+1,1)
 105 are single column arrays containing the coefficients in (3) that define the distributions of
 106 internal forces; and \mathbf{B} (k,n+1) are matrices which elements are the integrals resulting
 107 from the application of equation (1) generally or (2) for linear elastic materials.

108 Hence, equation (4) represents the general system of equations to be solved for \mathbf{C} . It
 109 must be noted that a different n may apply, in principle, for each internal force
 110 distribution (e.g. using the same number of coefficients for all distributions results in
 111 $4(n+1)$ unknowns). However, if only bending moments are considered, (4) can be
 112 written as

$$\begin{matrix} 113 \\ \end{matrix} \begin{bmatrix} u_1 \\ u_2 \\ \dots \\ u_j \\ \dots \\ u_k \end{bmatrix} = \begin{bmatrix} \int \frac{M_{(1)1}}{EI} dx & \int \frac{M_{(1)1}f_1(x)}{EI} dx & \dots & \int \frac{M_{(1)1}f_i(x)}{EI} dx & \dots & \int \frac{M_{(1)1}f_n(x)}{EI} dx \\ \int \frac{M_{(2)1}}{EI} dx & \int \frac{M_{(2)1}f_1(x)}{EI} dx & \dots & \int \frac{M_{(2)1}f_i(x)}{EI} dx & \dots & \int \frac{M_{(2)1}f_n(x)}{EI} dx \\ \int \frac{M_{(j)1}}{EI} dx & \int \frac{M_{(j)1}f_1(x)}{EI} dx & \dots & \int \frac{M_{(j)1}f_i(x)}{EI} dx & \dots & \int \frac{M_{(j)1}f_n(x)}{EI} dx \\ \int \frac{M_{(k)1}}{EI} dx & \int \frac{M_{(k)1}f_1(x)}{EI} dx & \dots & \int \frac{M_{(k)1}f_i(x)}{EI} dx & \dots & \int \frac{M_{(k)1}f_n(x)}{EI} dx \end{bmatrix} \begin{bmatrix} C_0 \\ C_1 \\ \dots \\ C_j \\ \dots \\ C_n \end{bmatrix} \quad (5)$$

114 where $M_{(j)1}$ is the unit-load bending moment distribution of the system with a unit-load
 115 applied at the position and in the direction of u_j .

116 Each row in equation (5) can hence be rewritten as

$$117 \quad u_j = \frac{1}{EI} \sum_{i=1}^{n+1} B_{ij} C_{i-1} \quad (6)$$

118 where $B_{i,j}$ represents each of the integrals shown in equation (5).

119 The system of equations in (5) was solved in MATLAB (2013) using the method of least-
 120 squares. The conditions for the system to have a unique solution are that $k > n+2$ and
 121 the rank of \mathbf{B} is greater than k . In general the first condition will always apply (e.g. for a
 122 pile under lateral load where its bending moment is approximated using a 4th order
 123 polynomial, $n=5$, k must be equal or greater than 7. This requirement is easily fulfilled in
 124 practice as the typical number of readings for an instrumented pile will traditionally
 125 exceed this number; the same typically applies to retaining walls and tunnels). The
 126 second condition was always fulfilled for the cases studied and should always be
 127 checked.

128 **APPLICATION TO RETAINING WALLS AND Laterally LOADED PILES**

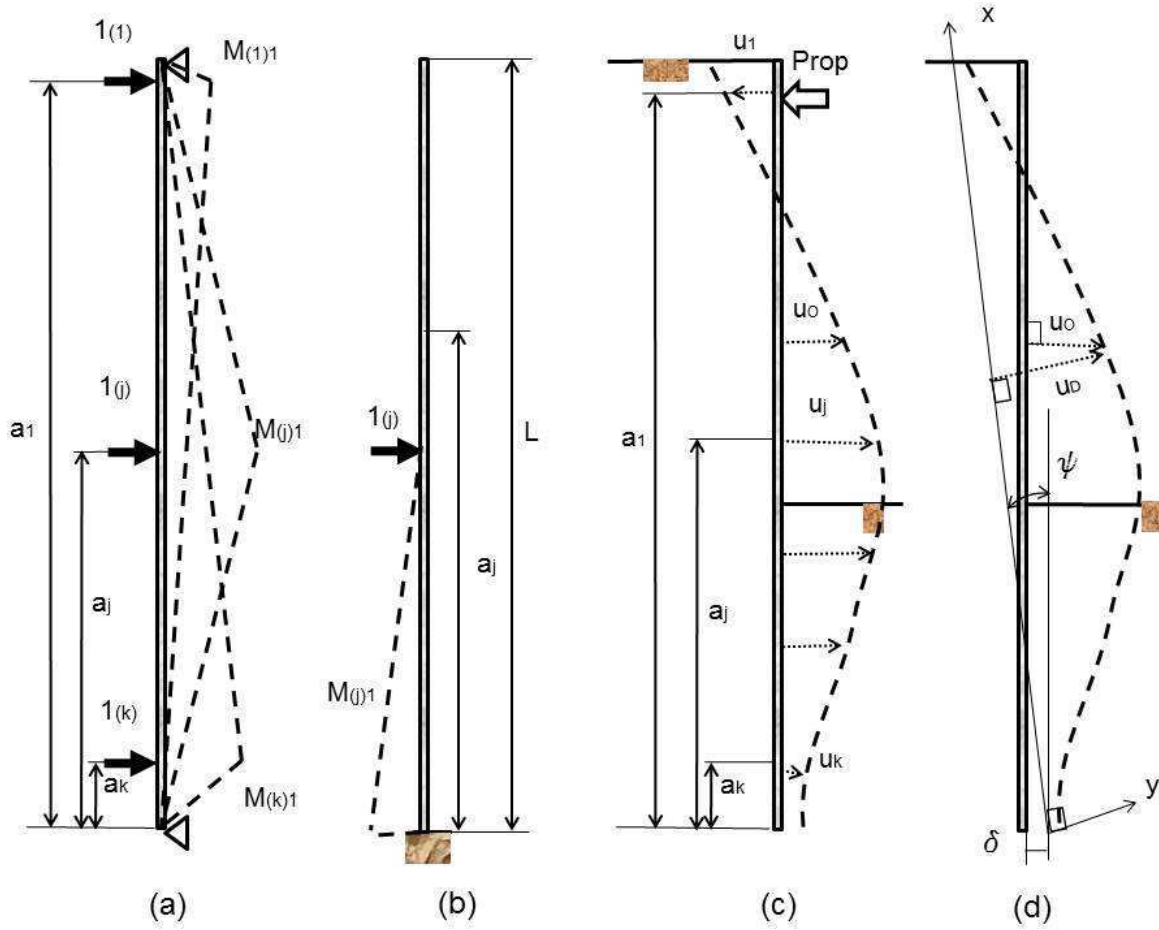
129 ***Assumptions***

130 The following general assumptions are made: linear elastic material behaviour applies;
 131 cross sections that are plane before deformation remain plane and; only small
 132 deformations are applied to the structure.

133 Since the focus for piles and retaining walls is on calculating bending moments, only the
134 displacements perpendicular to the pile / retaining wall longitudinal axis need to be
135 considered.

136 It is also assumed that bending moments are the dominating internal force in relation to
137 the above displacement and therefore, Eqs. (5) and (6) apply. This has been previously
138 confirmed by others like Anagnostopoulos and Georgidis (1993), who showed that the
139 axial load has a limited effect on the lateral displacement of piles and concluded that it
140 can be disregarded in static conditions, or Abdoun et al (2013) who also confirmed this
141 when showing that the presence of axial forces had little impact on lateral
142 displacements under seismic loading. Similarly, shear forces can be disregarded as
143 Gere & Timoshenko (1987) proved that their contribution to the lateral displacements is
144 small. Finally, the problems studied here are either plane strain or axisymmetrical
145 approximations, which means that torsion is also not relevant.

146 In order to apply (5) and (6), the real structures were idealised: propped walls as a
147 simply supported beam (Fig. 1a) and cantilever walls and laterally loaded piles as a
148 cantilever beam (Fig. 1b). Although these assumptions have been made by others –
149 e.g. Nig & Ng (2005) for laterally loaded piles – they are proposed and their validation is
150 part of this paper for more general conditions and geometries.



151 (a) (b) (c) (d)

152 **Figure 1. Piles and embedded retaining walls (a) UL for propped walls (b) UL for propped**
 153 **walls for cantilever walls and laterally loaded piles (c) Displacement definitions (d)**
 154 **Bending displacements**

155 Structural observed displacements (herein called u_0 - See Figure 1c) can be divided into
 156 three different main components (Gaba et al, 2003): rigid body rotation (ψ); rigid body
 157 translation (δ) and; bending (u_D) as illustrated in Figure 1d. Out of the three, only the
 158 latter contributes to the bending moments in the structure; hence, its isolation is needed
 159 for the application of the method and should be the only component to be used. In linear
 160 elastic behaviour, these can be superimposed which simplifies the process of sorting.

161

162 **Formulation**

163 Using polynomials of order n in equation (3) such as

164 $f_0(x) = 1, f_1(x) = x^1, \dots, f_n(x) = x^n$ (7)

165 and the unit-load bending moment distributions for propped walls

166
$$M_{(j)1}(x) = \begin{cases} \frac{L-a_j}{L}x, & x < a_j \\ -\frac{a_j}{L}x + a_j, & x \geq a_j \end{cases}$$
 (8)

167 and, similarly, for cantilever walls and laterally loaded piles (see Figure 1 for variable
168 definitions),

169
$$M_{(j)1}(x) = \begin{cases} a_j - x, & x < a_j \\ 0, & x \geq a_j \end{cases}$$
 (9)

170 the integrals in Eq. (5) and (6) become

171
$$B_{j,i} = \frac{L-a_j}{L} \frac{a_j^{i+2}}{i+2} + a_j \left(-\frac{L^{i+1}}{i+2} + \frac{L^{i+1}}{i+1} + \frac{a_j^{i+2}}{(i+2)L} - \frac{a_j^{i+1}}{i+1} \right)$$
 (10)

172 for propped retaining walls and

173
$$B_{j,i} = a_j \frac{a_j^{i+1}}{i+1} - \frac{a_j^{i+2}}{i+2}$$
 (11)

174 for cantilever walls and laterally loaded piles.

175 Equations (10) and (11) define the system of equations in (5) and (6) to be solved.

176 **Choice of function f(x)**

177 Multiple authors have chosen polynomials to approximate displacements and bending
178 moments of underground structures due to their versatility. However, the choice of order
179 is much less thoroughly explained in the literature and the reasons for choice are
180 normally justified by the amount of boundary conditions available, or a trial and error
181 procedure rather than a rigorous goodness-of-fit. A common mistake is to choose higher
182 order polynomials as they provide an apparent better fit to data; however, this may lead

183 to over-fitting and instabilities that are important, especially if the polynomials are used
184 to derive other parameters from its derivatives such as shear forces or soil reaction. de
185 Sousa (2006) proposed a sophisticated technique using polynomial splines in order to
186 solve this problem. The strategy proposed here to address the above problem is simple
187 and presented using Reese (1997) and Mohamad et al (2011) case studies (see Table
188 1 for description):

189 - First, the bending moments are calculated using multiple polynomial orders and Eq.
190 (5), (6), (10) and (11). Typical starting values of polynomial orders, based on
191 experience, are: 5th to 9th (Singly Propped walls), 6th to 10th (Multi-propped walls) and 4th
192 to 8th (Cantilever walls and laterally loaded piles). The above values of polynomial order
193 are only initial; iterations beyond those values may be necessary until the best order is
194 found as shown below.

195 - Model Evaluation –The Akaike Information Criterion (AIC) (Akaike, 1974) was used to
196 evaluate each polynomial. Later updates (Hurvich and Tsai, 1991), that correct for
197 models where the number of points is similar to the number of independent variables to
198 be estimated, were dismissed as it increases the risk of under-fitting (Bozogan, 1987).
199 The AIC approach provides a formulation that complies with the principle of parsimony,
200 by which the simplest model is selected, and eliminates the risk of over-fitting. AIC is
201 found using the following equation

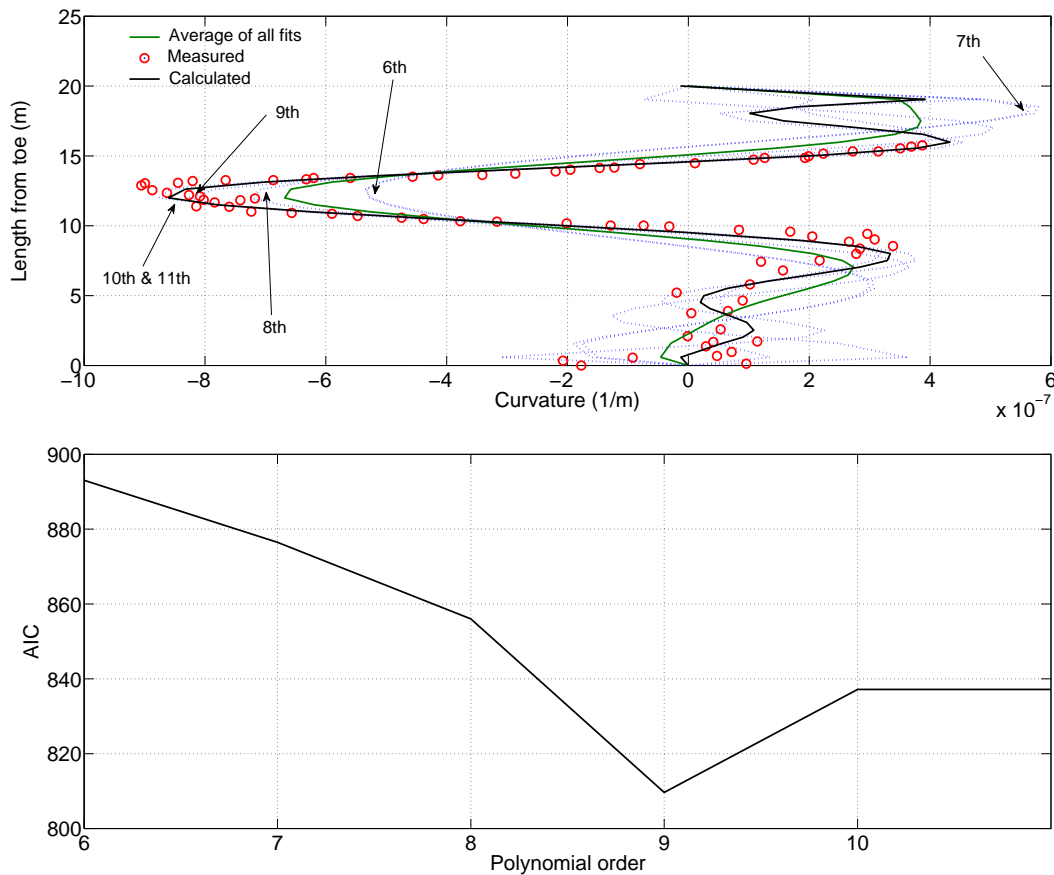
$$202 \quad AIC = -k * \text{LN} \left(\frac{SSE}{k} \right) + 2(n + 1) \quad (12)$$

203 where SSE is the Sum of Square of Errors defined as

$$204 \quad SSE = \sum_1^N (f_n - \hat{f})^2 \quad (13)$$

205 and f_n is the polynomial under evaluation, and \hat{f} is an estimator which is defined as the
 206 average of all the polynomials used.

207 Figures 2 and 3 show the implementation of Eq. (5) and this strategy. The optimal
 208 orders (lowest AIC score) are 9th for Mohamad et al (2011) and 6th for Reese (1997).
 209 When the lowest AIC value corresponds to the highest or lowest polynomial order
 210 considered initially, it will be necessary to reduce or increase the order until the
 211 minimum is found.



212

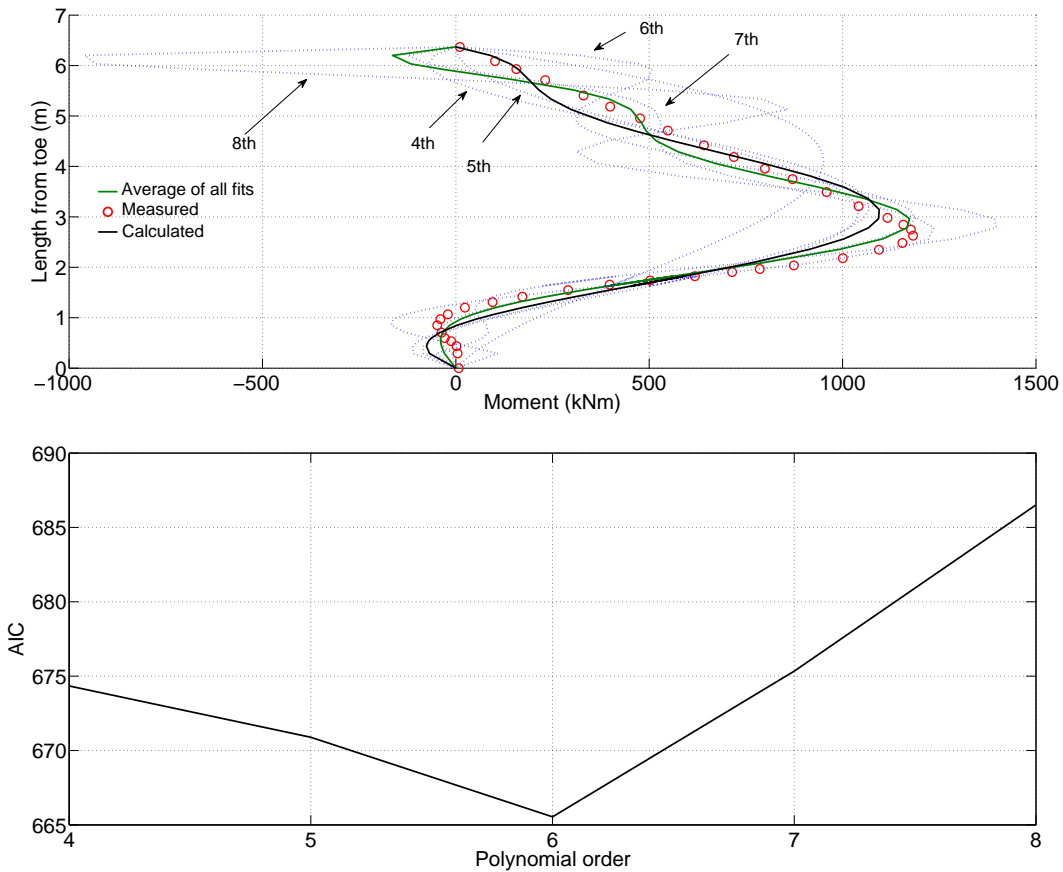
213

214 **Figure 2. Development of method for Mohamad et al (2011) (a) Polynomial choice (b) AIC**

215 - Once the best order has been chosen, the final solution is taken as the average of fits
 216 between the optimal polynomial order and the two closest orders with the lowest AIC
 217 score. It must be noted that the two closest may be on one side of the optimal. For

218 example, in Mohamad et al (2011), the optimal order is 9th and 10th and 11th have lower
 219 AIC scores than 8th. Hence, the final solution is taken as the average of polynomials of
 220 orders 9th, 10th and 11th.
 221 The above strategy was tested for all the cases in Table 1 as part of the validation
 222 process below. Appendix A shows its full application, including AIC plots for all the
 223 cases.

224



225

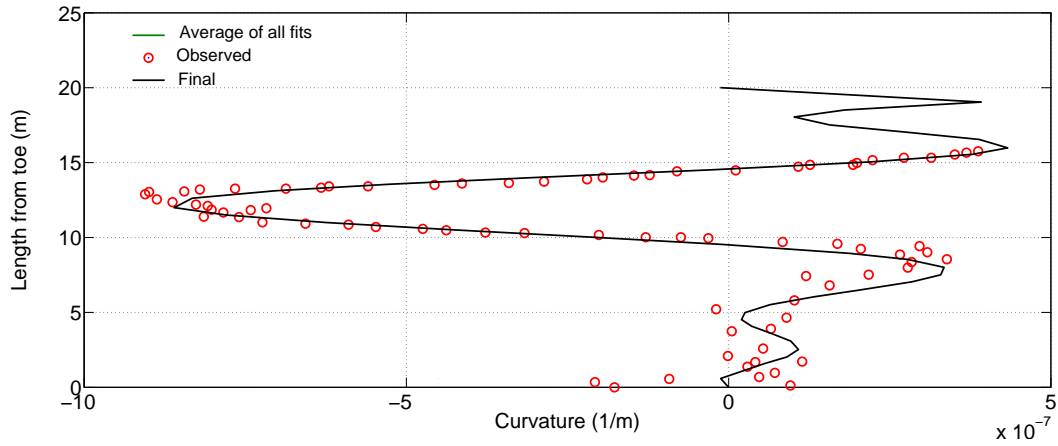
226 **Figure 3. Development of method for Reese (1997) (a) Polynomial choice (b) AIC**

227 **Validation**

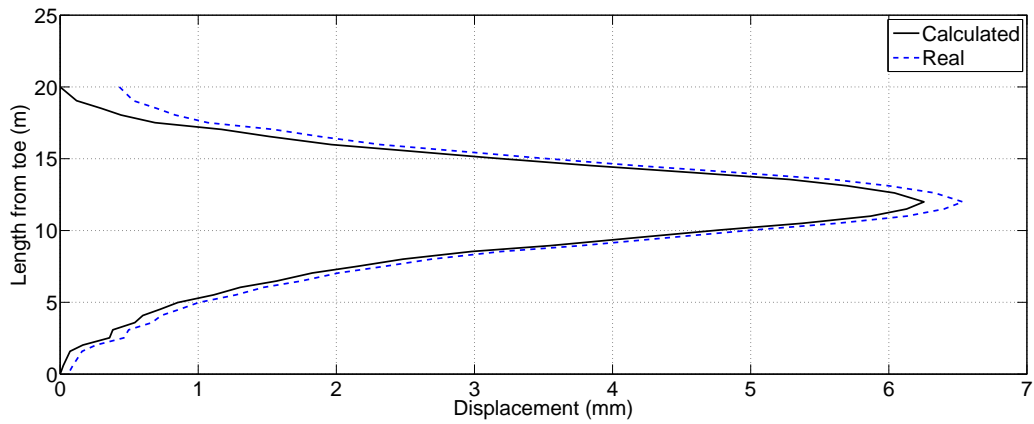
228 Six case studies (described in Table 1) were analysed to validate the method's
 229 application to piles and embedded retaining walls. They portray multiple loading
 230 conditions (earth pressures, tunnel induced load on piles, earthquake induced loads on

231 piles, to piles embedded in sliding embankments), structural dimensions and
232 construction methodologies and hence, cover a wide spectrum of situations.

233

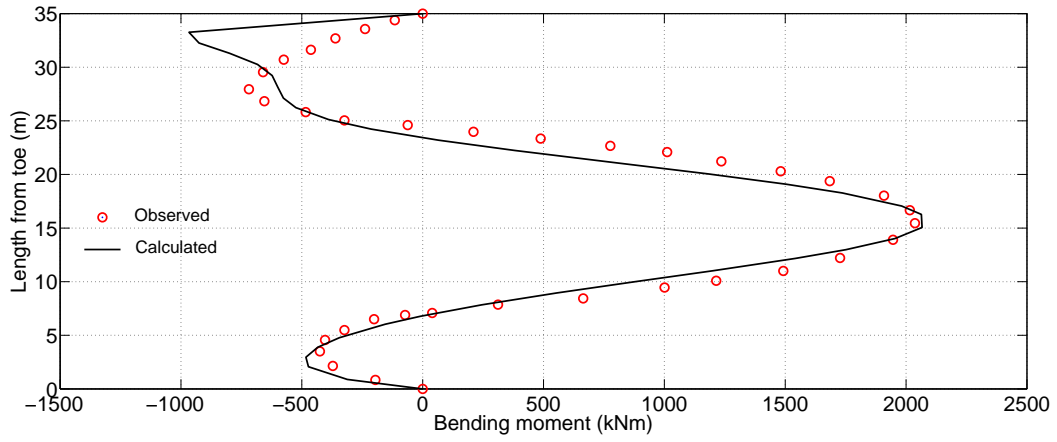


234

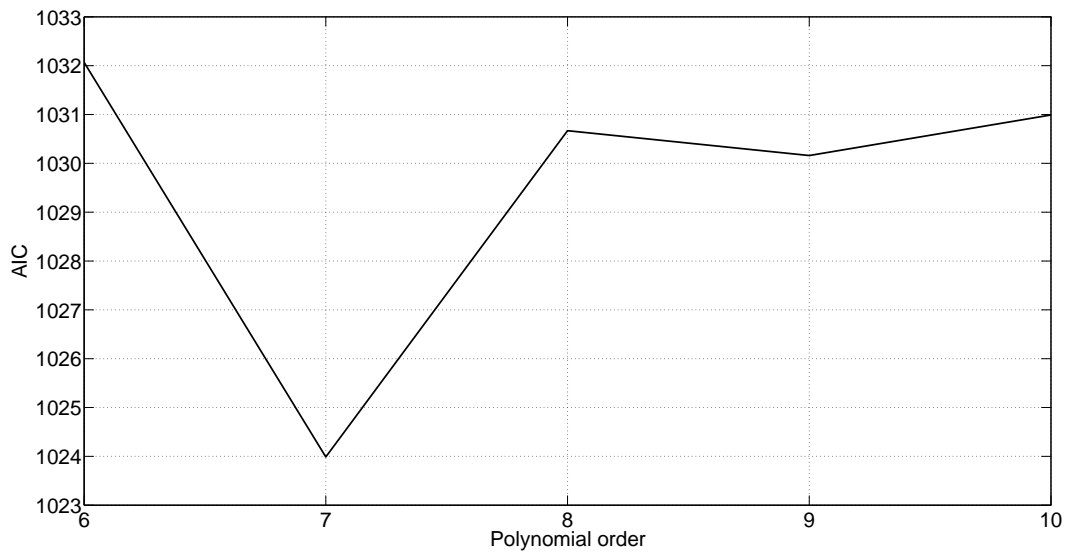


235 **Figure 4. Calculation (a) Curvature (b) Input displacement - Mohamad et al (2011)**

236

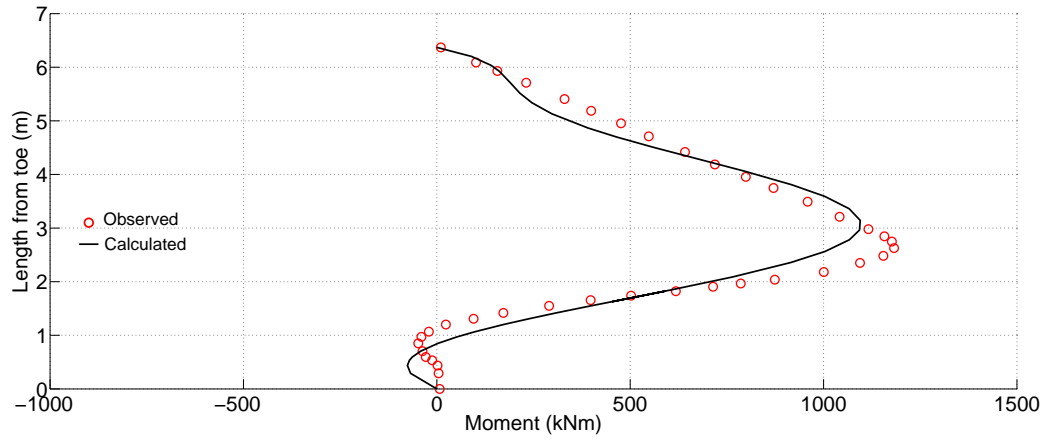


237

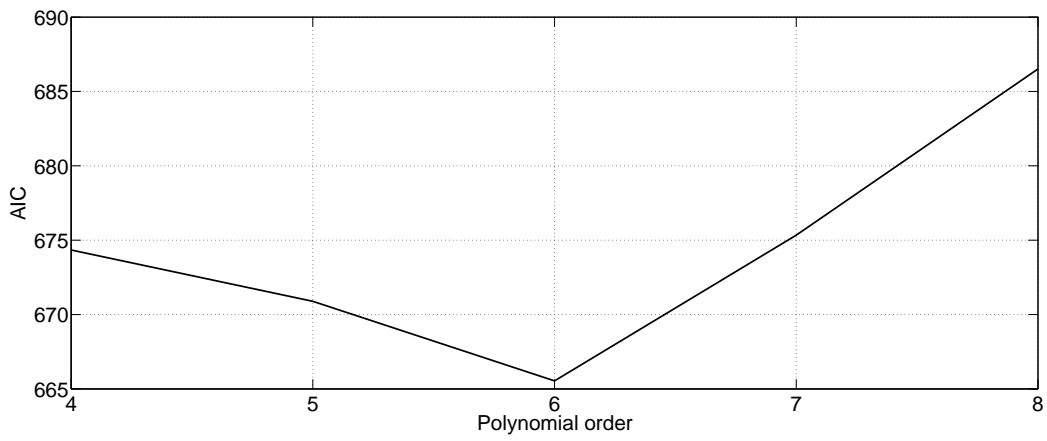


238 **Figure 5. Calculation (a) Bending moment (b) Input displacement - Ou et al (1998)**

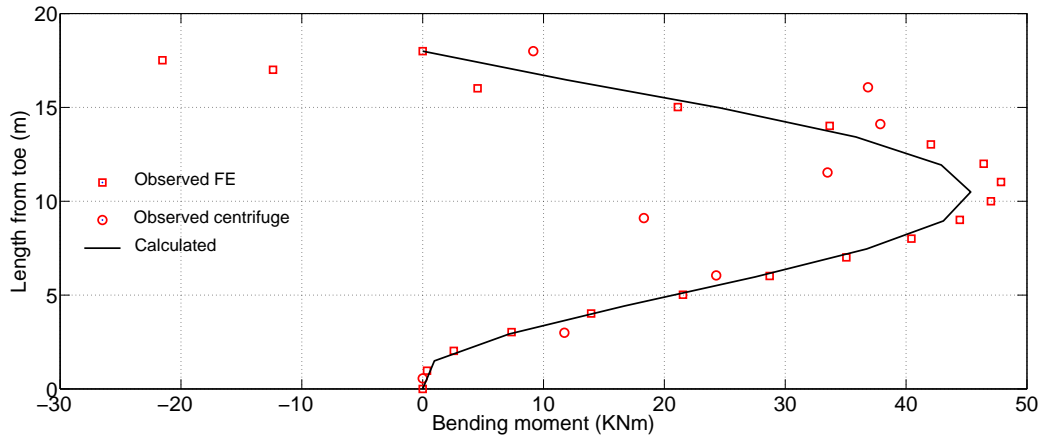
239



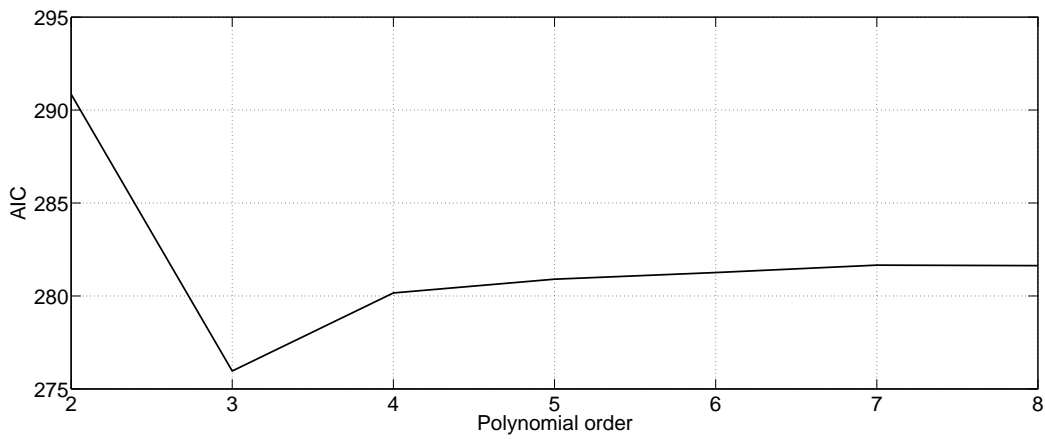
240



241 **Figure 6. Calculation (a) Bending moment (b) Input displacement - Reese (1997)**

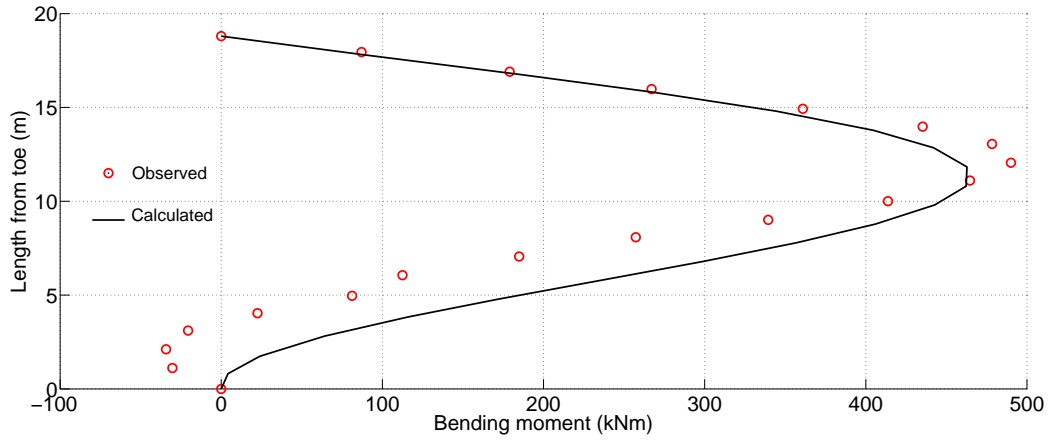


242

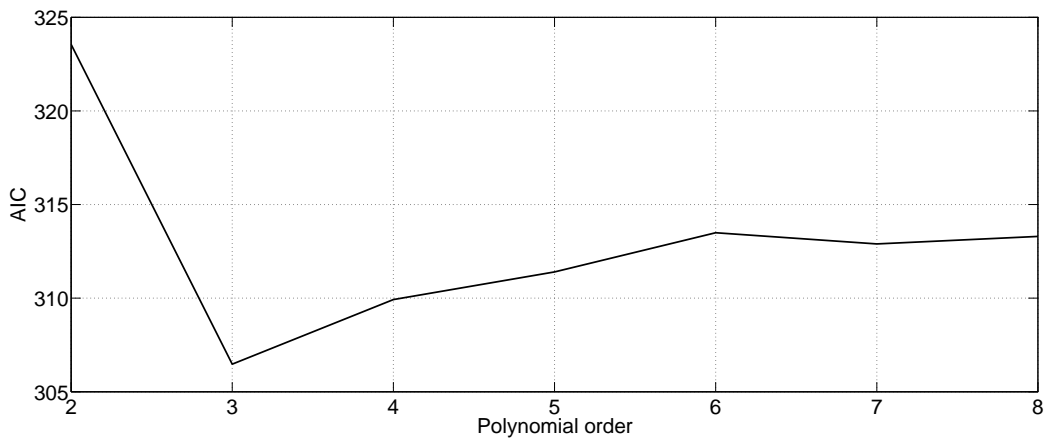


243

244 **Figure 7. Calculation (a) Bending moment (b) Input displacement - Cheng et al (2007)**



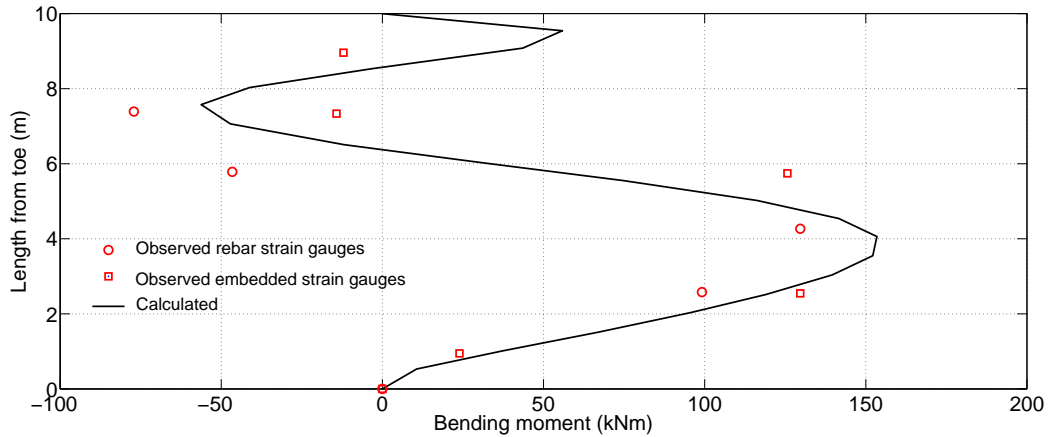
245



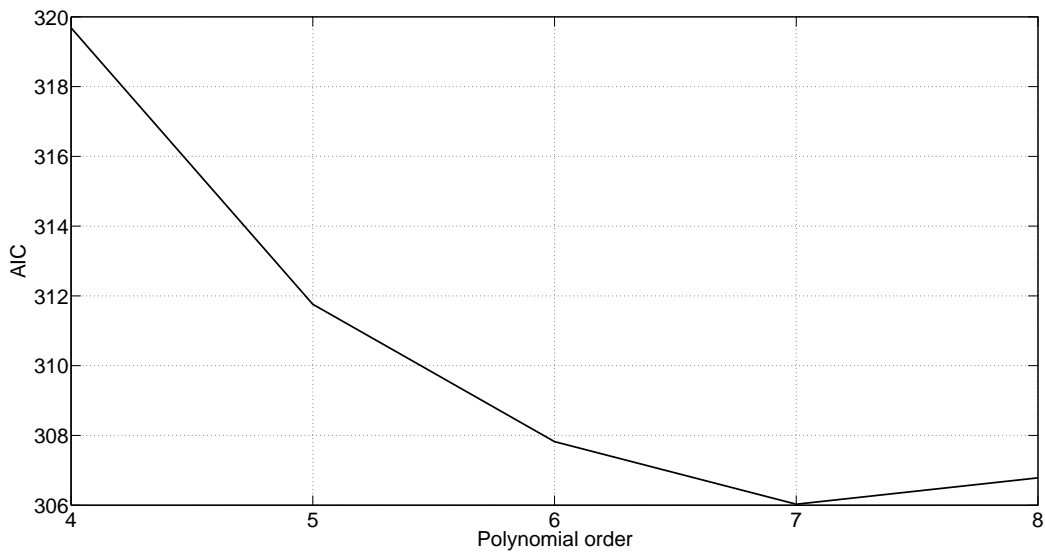
246

247 **Figure 8. Calculation (a) Bending moment (b) Input displacement - Liyanapathirana &**
 248 **Poulos (2005)**

249



250



251

252 **Figure 9. Calculation (a) Bending moment (b) Input displacement - Smethurst & Powrie**
 253 **(2007)**

254 Figures 4 to 9 show comparisons between the Calculated values (resulting from the
 255 method's application) and the Observed values (obtained from the literature). The
 256 figures also show the Input displacement and the Observed values to illustrate in which
 257 cases a transformation, like that shown in Figure 1d, was needed to calculate u_D .

258 The match between the maximum Observed values from the literature and the
 259 Calculated is within 10% for all cases, with the exception of Smethurst & Powrie (2007),
 260 which is 18%. It must be noted that in this case the value of EI that was used is only an

261 estimate by the authors for a stage where the pile is no longer behaving fully elastically.
262 It therefore confirms the potential of the method to predict bending moments beyond the
263 elastic range if the adequate value of EI is used.

264 The Calculated values deviate, in some instances (e.g. Ou et al, 1998) towards the
265 ends of the structure, typically, the upper part, which corresponds to where the
266 displacement readings, mostly done by inclinometers, accumulate the highest errors.
267 Therefore, this source of deviation cannot be simply attributed to the method as it is
268 more likely to be mostly due to inaccuracies in displacement measurements.

269 **APPLICATION TO TUNNELS**

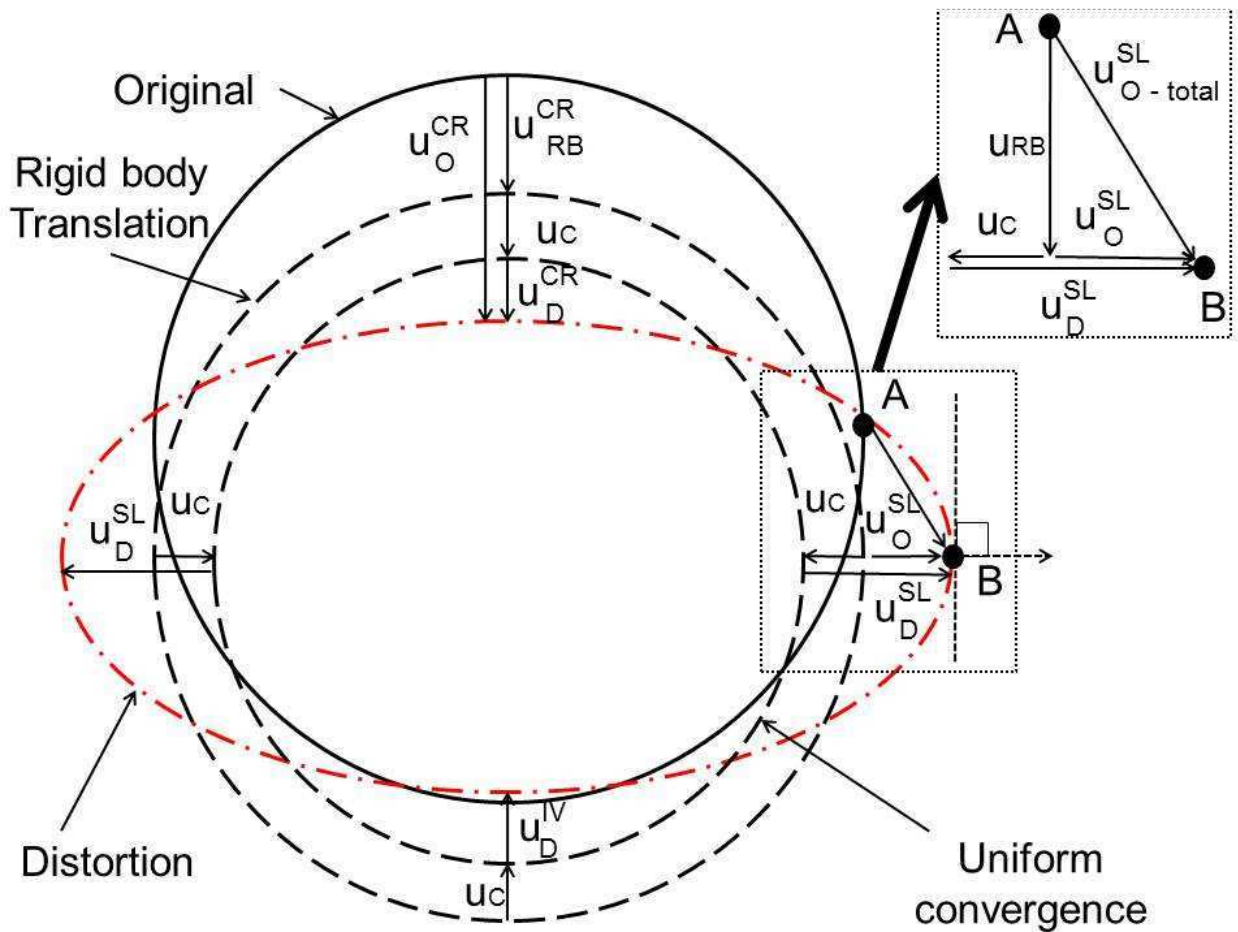
270 ***Assumptions***

271 The same general assumptions used for piles and retaining walls apply to tunnels.
272 Here, the focus is on circular tunnels for simplicity, although the same principles apply
273 to other section shapes. It is assumed that the tunnel lining structure is monolithic (i.e.
274 the joints are not articulated) and provides full structure continuity.

275 Furthermore, it is assumed that the ratio between the radius of the tunnel and its lining
276 thickness is greater than 7 approximately and therefore, the beam can be analysed
277 using straight beams deflection theory (Roark, 1965) - i.e. equation (2) applies. This
278 assumption also allows disregarding the effect of shear forces, as the structure can be
279 considered a thin shell.

280 Radial displacements, perpendicular to the tunnel cross section, were used (see Figure
281 10). The Observed displacements (u_O) can be, as in piles and retaining walls, divided
282 into two categories: those that produce bending moments and those that do not. The
283 latter, in practice, are rigid body (u_{RB}) displacements – i.e. a translation and / or rotation

284 - and uniform convergence (u_c) displacements – i.e. a uniform reduction in the tunnel
 285 diameter (see Figure 10). The former are displacements referred here as distortion
 286 displacements (u_D) – typically ovalisation; however, other potential displacements such
 287 as those arising from gaps behind the lining or localised loading must also be included
 288 (the example shows only ovalisation deformations for simplicity). It is important to note
 289 that everything that follows applies to the rotated tunnel, which means that if a rigid
 290 body rotation has occurred, it needs to be removed from the observed values in
 291 advance to present it as it is shown in Figure 10.



292
 293 **Figure 10. Tunnel displacements definitions**

294

295 Having made the above distinction, the general equation for the radial displacements
296 can be written as

$$297 \quad u_O = u_{RB} + u_C + u_D \quad (14)$$

298 where u_O represents the Observed radial displacements of the rotated tunnel and u_{RB} is
299 the projection of the rigid body displacement onto the radial direction for each point (e.g.
300 if the rigid body displacement is a vertical translation as in Figure 10, the tunnel crown
301 u_{RB} is the Observed total rigid body displacement value, whereas in the springline this
302 value is zero). The sign convention in Eq. (14) is: negative for radial displacements
303 acting inwards and positive for those acting outwards.

304 The uniform convergence and rigid body displacements do not cause a change in
305 shape (i.e. the normal to tunnel lining does not change direction), which means there is
306 no shear deformation, and no bending moment. Therefore, if the normal to the tunnel at
307 the springline remains horizontal after deformation, it follows that the distortion
308 displacement at this location must also be horizontal. It also means that the vertical
309 component of the rigid body displacement is equal to the vertical component of the
310 observed displacement. Hence, if the same horizontal component of the observed
311 displacement applies at both springlines and in opposite directions, the rigid body
312 displacement must be vertical (as is the case presented in Figure 10). This reasoning
313 applies to any tunnel as long as the lining acts as a monolithic material with no joints.

314 Uniform convergence can be obtained by inspecting the tunnel cross section
315 displacements at the crown (CR) and the springline (SL) and developing (14) for each

$$316 \quad u_O^{SL} - u_{RB}^{SL} = u_C + u_D^{SL} \quad (15)$$

$$317 \quad u_O^{CR} - u_{RB}^{CR} = u_C + u_D^{CR} \quad (16)$$

318 In Figure 10, the distortion deformation of the example is elliptical and therefore, Eq.
 319 (15) refers to displacements in the horizontal direction and (16) in the vertical direction.

320 Using the ratio between the crown and springline distortion deformations, u_D^{CR}/u_D^{SL} ,
 321 substituting this into Eq. (15) and (16), subtracting algebraically both eliminates u_C , and
 322 isolating u_D^{SL} results in

$$323 \quad u_D^{SL} = \frac{u_O^{SL} - u_{RB}^{SL} - u_O^{CR} + u_{RB}^{CR}}{(1 - u_D^{CR}/u_D^{SL})} \quad (17)$$

324 and inserting (17) into (15) provides the uniform convergence

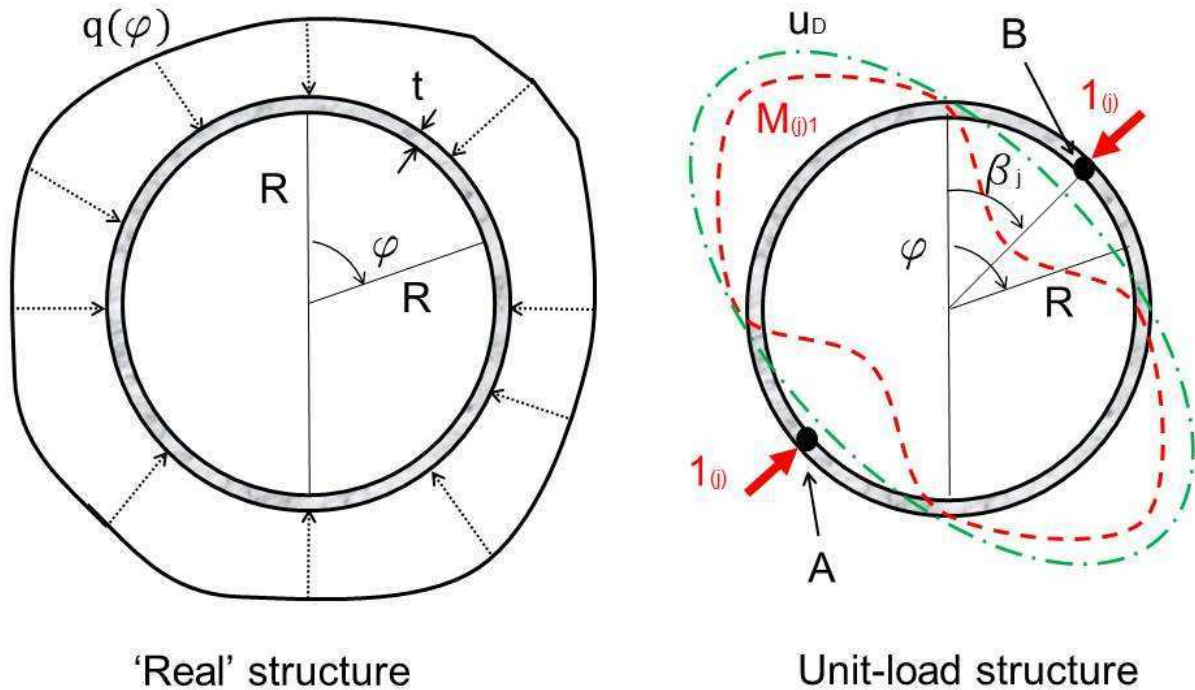
$$325 \quad u_C = u_m^{SL} - u_{RB}^{SL} - \frac{u_O^{SL} - u_{RB}^{SL} - u_O^{CR} + u_{RB}^{CR}}{(1 - u_D^{CR}/u_D^{SL})} \quad (18)$$

326 This value can then be used in Eq. (14) to calculate the final distortion displacements at
 327 any point in the lining

$$328 \quad u_D = u_O - u_{RB} - u_O^{SL} + u_{RB}^{SL} + \frac{u_O^{SL} - u_{RB}^{SL} - u_O^{CR} + u_{RB}^{CR}}{(1 - u_D^{CR}/u_D^{SL})} \quad (19)$$

329 Other methods can be used to separate sources of Observed displacements. What is
 330 important is to make sure that all displacements that do not produce bending moments
 331 are removed in preparation for the method's application. However, the methodology
 332 presented here is deemed applicable to most cases of standard displacements in
 333 tunnels and has been validated.

334 The idealisation needed for the application of the method to tunnels is shown in Figure
 335 11. It consists of a thin ring with a double unit-load applied in diametrically opposite
 336 locations.



337

338 **Figure 11. Tunnel nomenclature definition and idealisation and unit-load structure**

339 **Formulation**

340 The chosen function to represent the real structure bending moments and axial forces is
 341 shown below

$$342 \quad f_0(x) = 1, f_1(x) = \cos(\varphi), f_2(x) = \cos(2\varphi) \quad (20)$$

343 which is much simpler than for piles and retaining walls as it contains only three
 344 constants C (see Eq. 6) to calculate.

345 The distribution of bending moments for a generic unit-load system applied at an angle
 346 β_j was calculated generically for any angle ε , using the equations developed by
 347 Lundquist and Burke (1936)

$$348 \quad M_{(j)1}(\varphi) = \begin{cases} X_{(j)m} + R(1 - \sin(\varphi))X_{(j)p} + R \sin(\varphi)X_{(j)v}, & \varphi < \beta_j \\ R \sin(\varphi - \beta_j) + X_{(j)m} + R(1 - \sin(\varphi))X_{(j)p} + R \sin(\varphi)X_{(j)v}, & \varphi \geq \beta_j \end{cases} \quad (21)$$

349 where φ varies between 0 and 180°, and

$$350 \quad X_{(j)m} = R \frac{\left(\frac{\pi \sin(\beta_j)}{2} + 2\right)^{-3}}{\pi} \quad (22)$$

$$351 \quad X_{(j)p} = \frac{2 - \left(\frac{\pi \sin(\beta_j)}{2} + 2\right)}{\pi} \quad (23)$$

$$352 \quad X_{(j)v} = \frac{\cos(\beta_j)}{2} \quad (24)$$

353 Using Eq. (20) to (24), similar equations to (10) and (11) can be derived for tunnels as
354 follows

$$355 \quad B_{j,0} = \pi X_{(j)m} + \pi R X_{(j)p} - 2R X_{(j)v} + R(\cos(\beta_j) + 1) \quad (25)$$

$$356 \quad B_{j,1} = X_{(j)m} \sin(\beta_j) - X_{(j)p} R \frac{\sin(2\beta_j)}{2} - \frac{R \sin(\beta_j)(\pi - \beta_j)}{2} \quad (26)$$

$$357 \quad B_{j,2} = \frac{2}{3} R X_{(j)v} - \frac{R}{3} (\cos(\beta_j) + 1)(2\cos(\beta_j) - 1) \quad (27)$$

358 which allows redefining Eq. (6)

$$359 \quad u_{Dj} = \frac{R}{EI} \sum_{i=1}^{n+1} B_{ij} C_{i-1} \quad (28)$$

360 that represents the system equations from which the bending moments' constants of
361 equation (20) can be calculated.

362 Equations (6) and (28) are almost identical with the exception of the addition of R in the
363 latter, which comes from the integration using polar coordinates and the angle φ .

364 The same process applies to the axial force. In this case, the axial force caused by the
365 unit-load is

$$366 \quad N_{(j)1}(\varphi) = \begin{cases} -\frac{1}{2} \sin(\beta_j - \varphi), & \varphi < \beta_j \\ -\frac{1}{2} \sin(\varphi - \beta_j), & \varphi \geq \beta_j \end{cases} \quad (29)$$

367 Using Eq. (20) and (29), the integrals in (6) become

$$368 \quad B_{j,0} = 1 \quad (30)$$

$$369 \quad B_{j,1} = (2\beta_j - \pi)/4 \quad (31)$$

$$370 \quad B_{j,2} = -(2 \cos^2 \beta_j - 1)/6 \quad (32)$$

371 and the system of equations is defined as

$$372 \quad mu_{Dj} = \frac{R}{EA} \sum_{i=1}^{n+1} B_{ij} C_{i-1} \quad (33)$$

373 The factor m shown in (33) represents the fact that only a marginal contribution of the
374 distortion movements applies to the axial forces. The majority of the axial force is a
375 consequence of the displacement u_C and can be calculated as

$$376 \quad N_C = \frac{((R+u_C)-R)}{R} EA \quad (34)$$

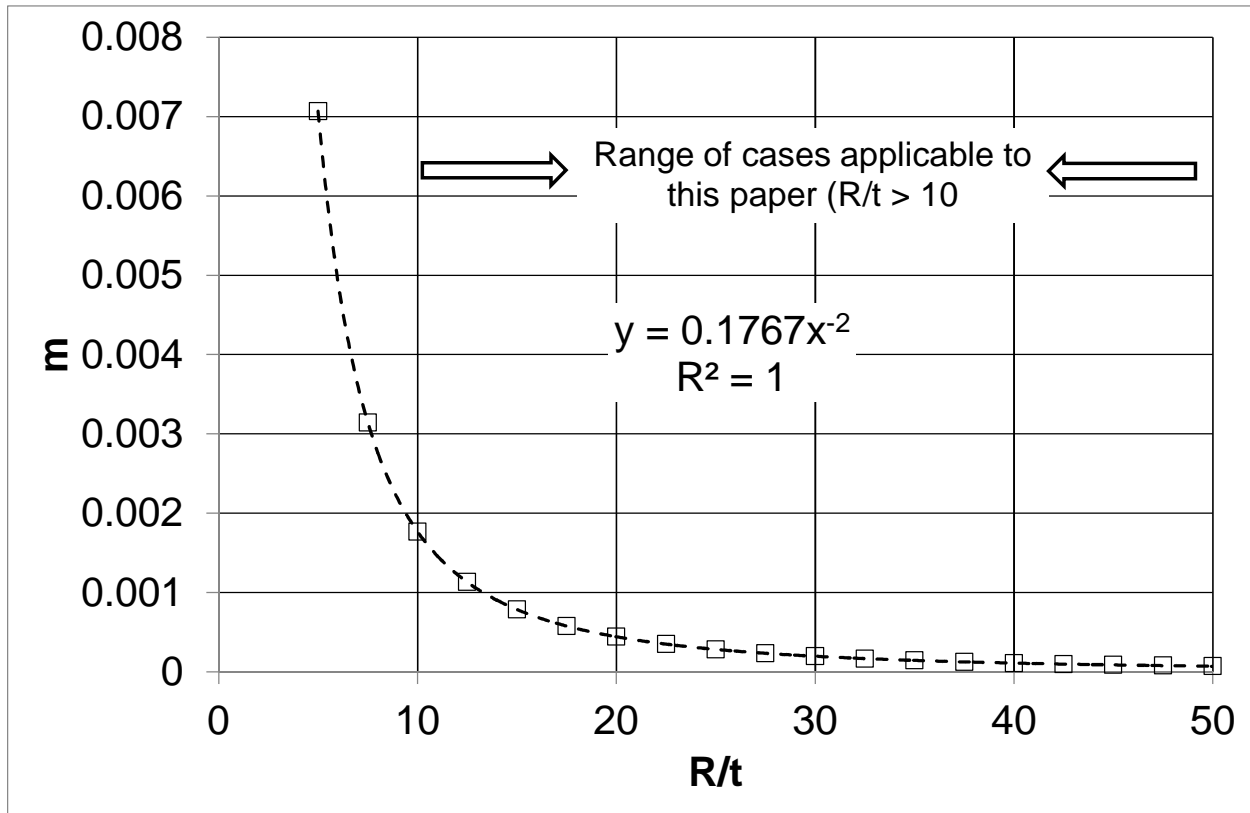
377 so that the final axial load is the summation of N_C (which is a constant load) and the
378 axial load calculated using Eq. (33) that varies for different points in the lining.

379 The factor, m , can be estimated ignoring the contribution of the shear forces and using
380 the radial displacement solution presented by Gere & Timoshenko (1987)

$$381 \quad u_D = \frac{\pi PR}{4EA} \left(12 \left(\frac{R}{t} \right)^2 + 2.12 \right) \quad (35)$$

382 The second term of the equation corresponds to the axial force contribution, and the
383 first to the bending moments. Figure 12 shows the power law that fits perfectly the ratio
384 between both contributions, m , when plotted against R/t ratio. Although Eq. (35) and
385 consequently, Figure 12, correspond to the case of a point load applied at the crown of
386 the lining, other combinations of external applied loads result in very similar power laws
387 and hence, the hypothesis was that the power law presented here can be used for

388 estimation purposes where the deformation of the tunnel is mainly elliptical. This
 389 hypothesis is validated below for both case studies.



390
 391 **Figure 12. Ratio between axial force and bending moment contributions to radial**
 392 **displacements**

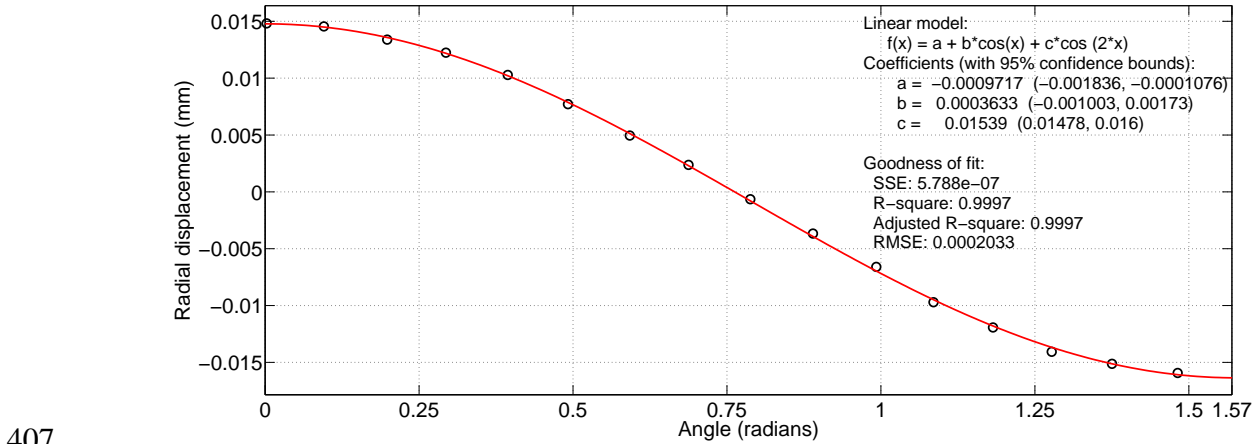
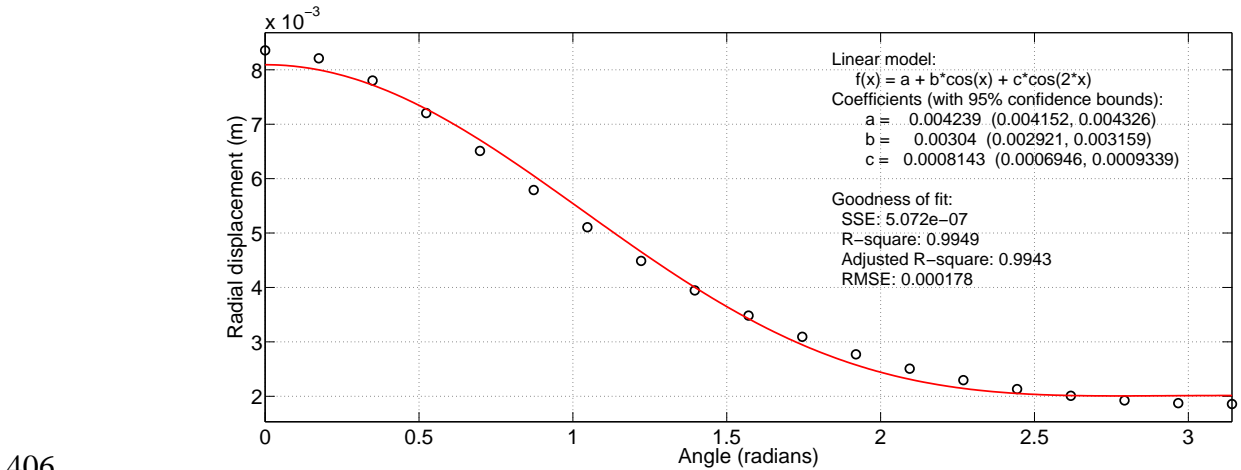
393 ***Choice of function f(x)***

394 Most of the widely accepted solutions for tunnel lining design define the shape of
 395 bending moments and radial displacements in tunnels using multiples of the cosine –
 396 e.g. $\cos(2\xi)$ (Einstein & Schwartz, 1979; El Naggar et al, 2008; Carranza-Torres, 2013)
 397 for simpler modes of deformation and $\cos(p\xi)$ for different orders, where p is an integer
 398 greater than 1 (Muir Wood, 1975).

399 Gere & Timoshenko (1987) showed that the equation linking radial displacement and
 400 bending moment of a circular beam of thin section is

401
$$\frac{d^2 u_D}{d\varphi^2} + u_D = -\frac{R^2 M(\varphi)}{EI} \tag{36}$$

402 which means that it is mathematically proven that if a function shape of the form shown
 403 in (20) could be successfully fitted to the displacement profile u_D , the same form would
 404 apply to the bending moments, provided that EI remains constant (as it does for the
 405 linear elastic region under consideration).



407
 408 **Figure 13. Validation of function choice (a) Gonzalez & Sagaseta (2001) (b) Carranza-**
 409 **Torres et al (2013).**

410 Figure 13 shows the fitted proposed function in Eq. (20) to the displacement profiles
 411 suggested by Gonzalez & Sagaseta (2001) and Carranza-Torres et al (2013) using the
 412 MATLAB (2013) curve fitting tool. The former presents a profile where symmetry occurs

413 around the vertical axis (note the x axis extends to 180°), whereas in the latter, double
414 symmetry occurs at 90° and subsequently at 180° .

415 Besides the discussion on the appropriateness of one method or another, which is
416 beyond the scope of this paper, the figure shows that the chosen function performs well
417 for both cases and provides very high values of R^2 and low of RMSE, indicating an
418 acceptable goodness-of-fit. This, in turn, shows that the function is also appropriate to
419 characterise bending moments: a similar rationale applies to axial forces.

420 **Validation**

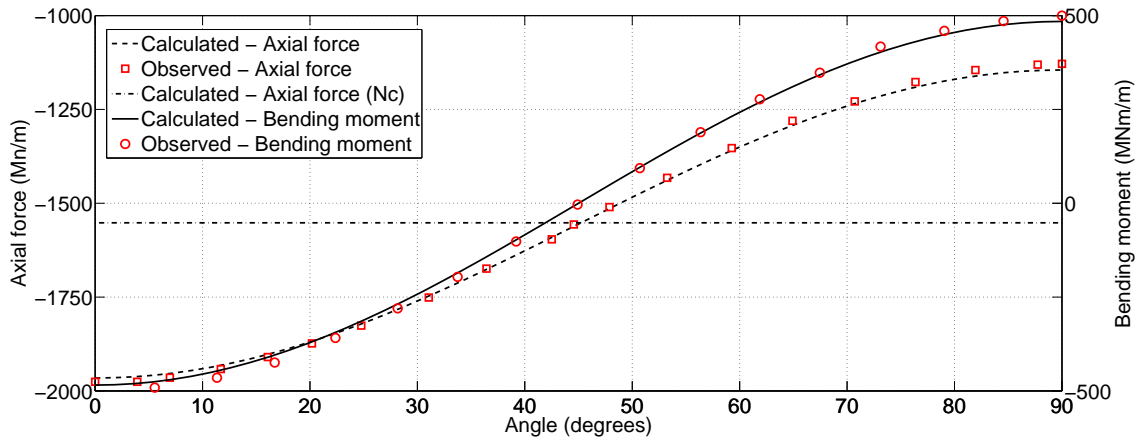
421 The validation was carried out against an analytical method such as Carranza-Torres et
422 al (2013) and an FE model in Brinkgreve et al (2011). The former is a more generalised
423 and complex case than those presented previously by others (e.g. Einstein & Schwartz,
424 1976) and includes complex processes such as stress relaxation. The second case is
425 representative of an accurate and calibrated FE model and programme widely used.
426 Details on both of these are presented in Table 1.

427 In order to separate the displacements, first an estimate of u_D^{CR}/u_D^{SL} is needed. In cases
428 where the rigid body translation is small compared to the maximum distortion
429 deformations (as is the case in most tunnels), it can be estimated as u_O^{CR}/u_O^{SL} . Hence,
430 u_D^{CR}/u_D^{SL} values of -1.027 and -1.099 were estimated for Brinkgreve et al (2011) and
431 Carranza-Torres et al (2013) respectively. This estimate was tested through a sensitivity
432 analysis of its impact on the calculation of bending moments using the value of pure
433 shear, -0.5, and extreme values ranging between -0.92 to -1.08 (calculated from Roark
434 (1965) for the case of a triangular horizontal pressure applied on the sides). Differences
435 of less than 0.5% in the Calculated bending moment were obtained which confirmed the

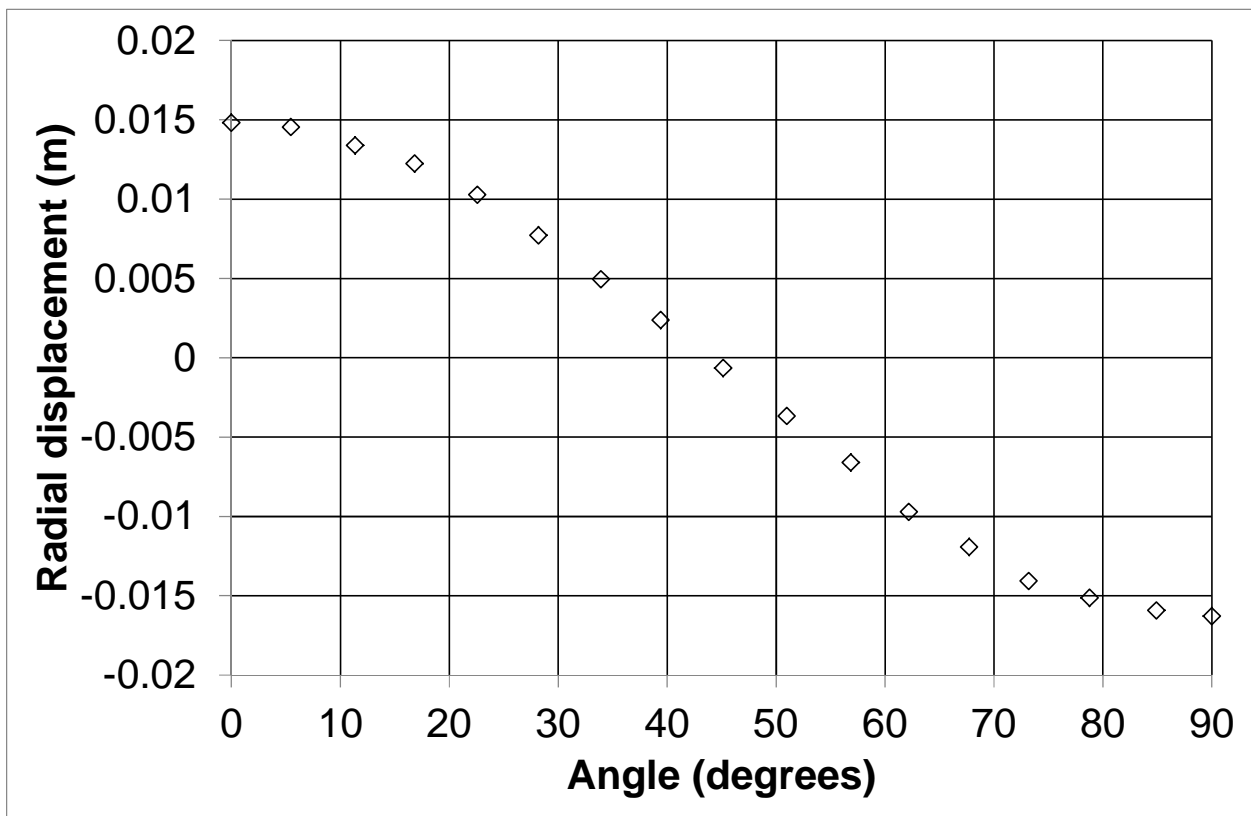
436 adequacy of the estimate. Eq. (18) was then used to calculate u_C , providing values of -
437 1.383E-0m and -6.208E-04m for Brinkgreve and Carranza-Torres respectively. Finally,
438 Eq. (19) was used to calculate u_D .

439 Using Eq. (34) and the calculated u_C value, N_C was obtained and was equal to -
440 774.79kN/m (Brinkgreve et al, 2011) and -1552 kN/m (Carranza-Torres et al, 2013). The
441 m values, were estimated using the equation in Figure 14, and were 3.460E-03 and
442 1.767E-03 respectively. This allowed calculating the contribution of u_D that corresponds
443 to the axial forces.

444 Figures 14 and 15 present the results of the method's application and its comparison to
445 the observed values. The match to Carranza-Torres et al (2013) is outstanding as the fit
446 is within 0.5%. For Brinkgreve et al (2011), the method captures the fact that the
447 bending moment is marginally higher at the crown of the tunnel than at the invert, and
448 only over-predicts the latter by 14%. The Calculated axial force is closer to the
449 Observed values and only shows an error of less than 5% for its maximum values at 0
450 (and 180) and 90 degrees respectively.



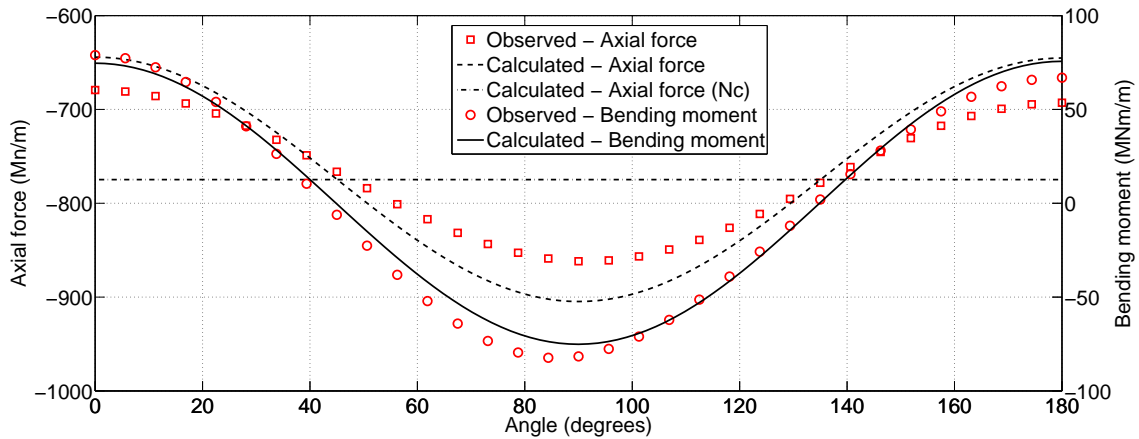
451



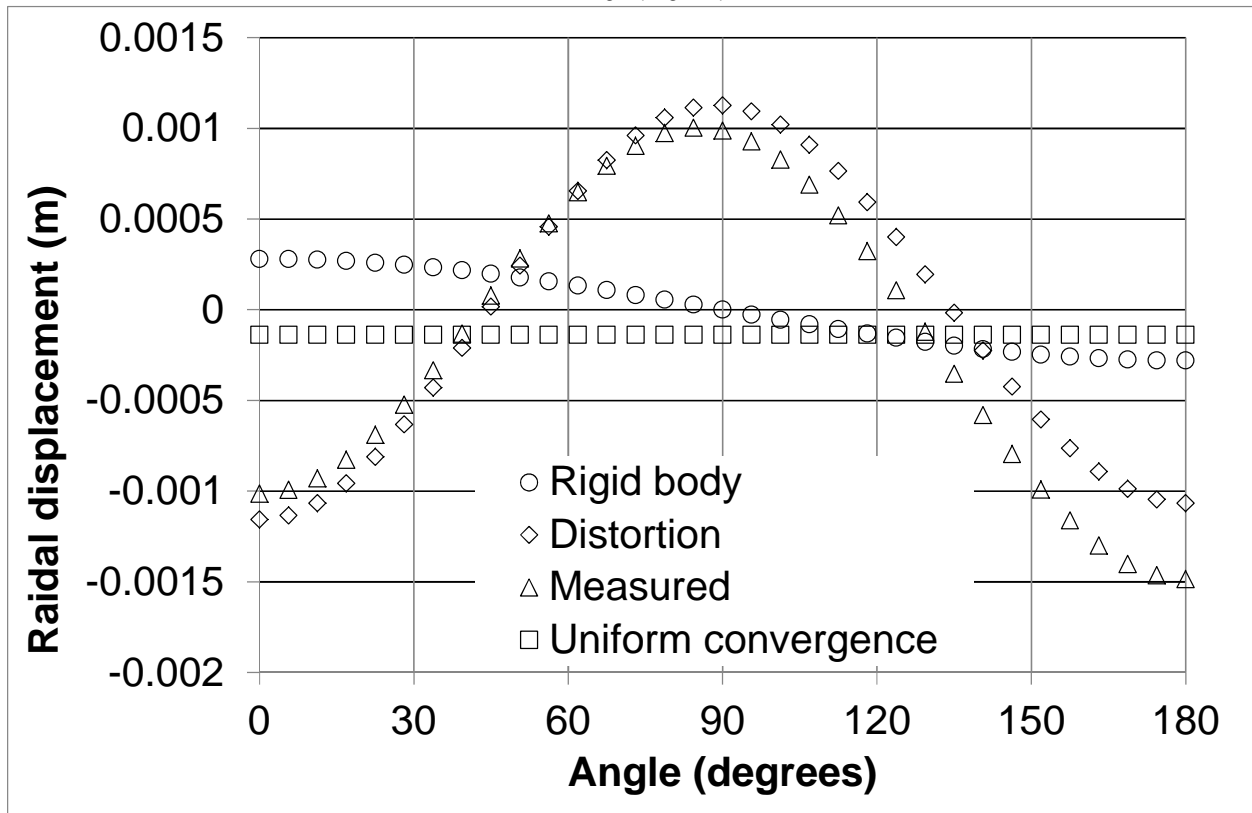
452

453 Figure 14. Calculation of (a) Bending moment and Axial force (b) Input radial

454 displacement - Carranza-Torres (2013)



455



456

457 **Figure 15. Calculation of (a) Bending moment and Axial force (b) Input displacements -**

458 **Brinkgreve et al (2011)**

459 Close inspection of Figures 14 and 15 also shows that N_C is the arithmetic average of

460 the axial load for both cases and the deviation from this average is the axial load that

461 arises from the displacements μ_D . This deviation is also indicative of the ratio between

462 the vertical and horizontal stresses acting on the tunnel lining, as Carranza-Torres and

463 Diederichs (2009) showed, which may present future opportunities for the estimation of
464 this ratio.

465 The outstanding performance of the method against very different case studies not only
466 validates it but also the procedure presented for the separation and reasoning of the
467 different displacements contributions.

468 **CONCLUSIONS**

469 The proposed method is analytically correct and based on the principle of virtual work. It
470 provides a means to calculating internal forces such as bending moments and axial
471 forces without the need for boundary conditions. It solves therefore a long standing
472 problem in underground structures that has significant applications in research and
473 practice as it provides an accurate and independent check on the internal forces in a
474 structure. This is envisaged to allow producing more optimised design though greater
475 understanding of the bending moments and axial forces in underground structures.

476 The versatility and flexibility of the method has been demonstrated using diverse case
477 studies which shows it is equally applicable to piles, retaining walls and tunnels under
478 multiple loading conditions. The maximum error between Observed and Calculated
479 values of bending moment was lower than 10%, with the exception of the case where
480 slight plastic behaviour occurred and the error was 18%.

481 The method presents multiple opportunities for future work and its relevance extends
482 beyond underground structures as the same methodology is theoretically applicable to
483 any structure. Therefore, its applicability and potential usage is wide.

484

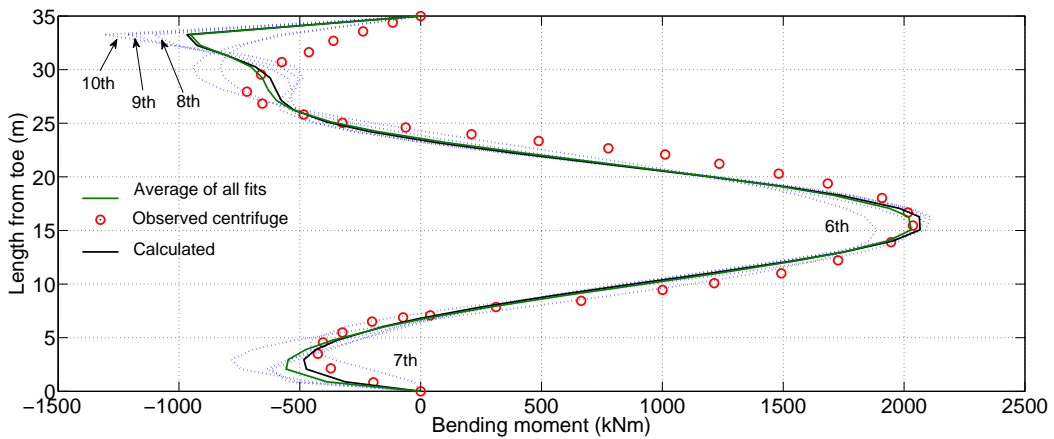
485

486 **ACKNOWLEDGMENTS**

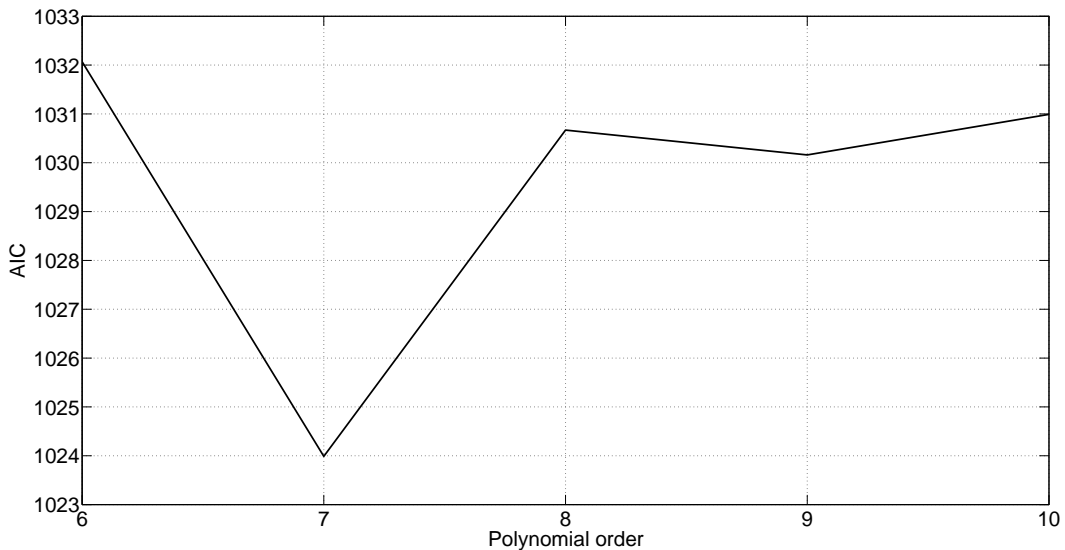
487 The author would like to acknowledge the discussions he had and recommendations
488 received from Eden Almog (Arup Tunnelling, London) throughout the derivation of the
489 method from its original idea. It is also acknowledged the suggestions that Loretta von
490 der Tann (University College London and Arup Geotechnics) made on the part dealing
491 with piles and retaining walls and the general presentation of the paper.

492 **APPENDIX A**

493 This appendix shows the full application of the method to all the case studies presented
494 for piles and retaining walls.

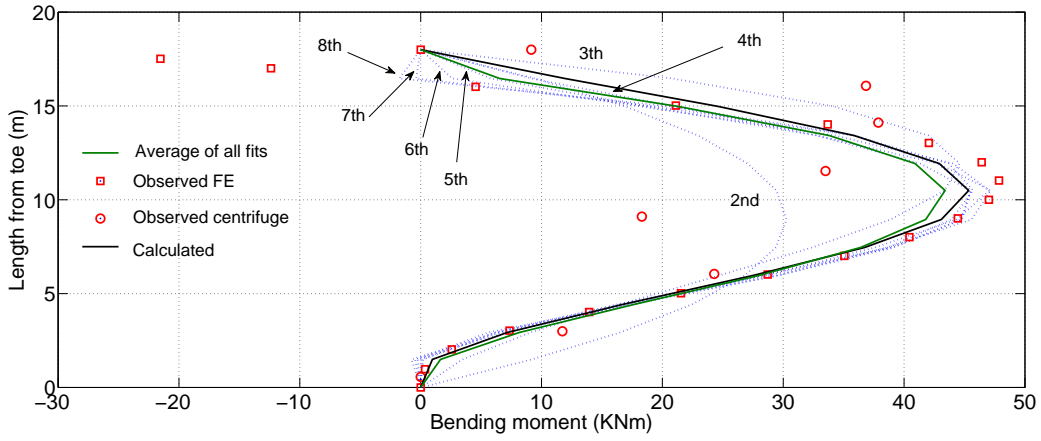


495



496

497 **Figure A1. Development of method for Ou et al (1998) (a) Polynomial choice (b) AIC**



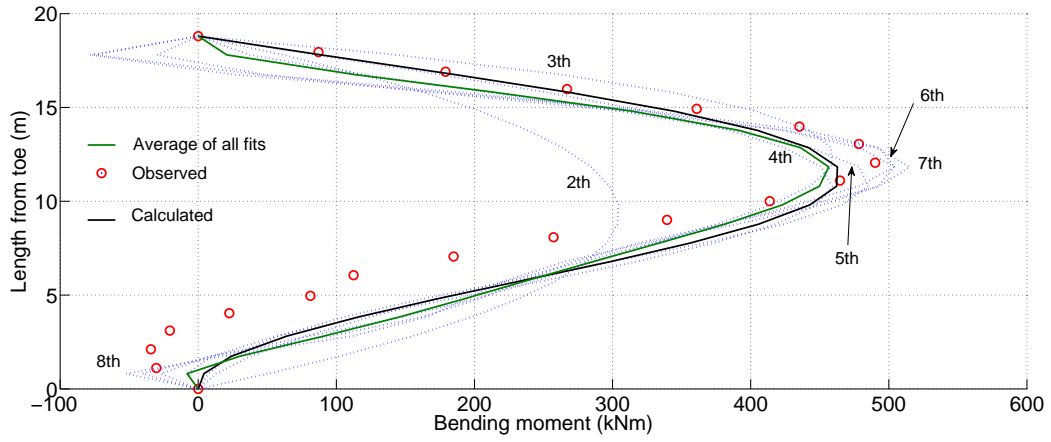
498



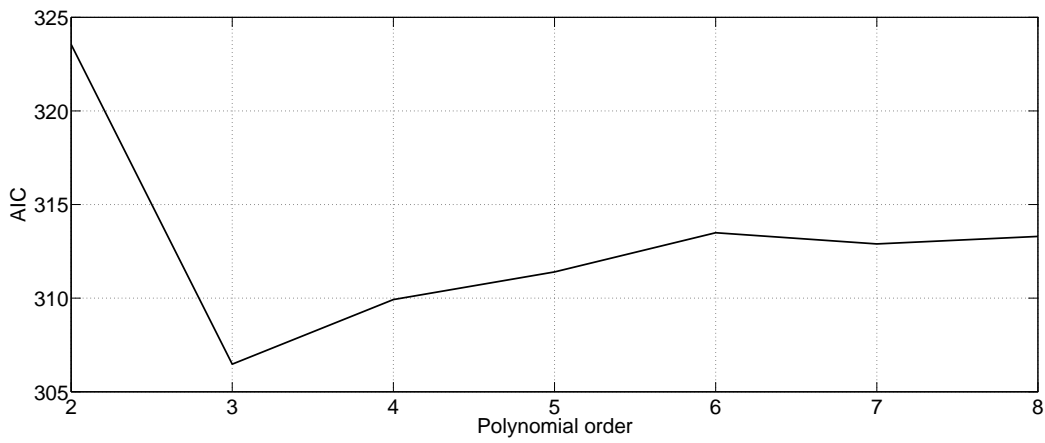
499

500 **Figure A2. Development of method for Cheng et al (2007) (a) Polynomial choice (b) AIC**

501



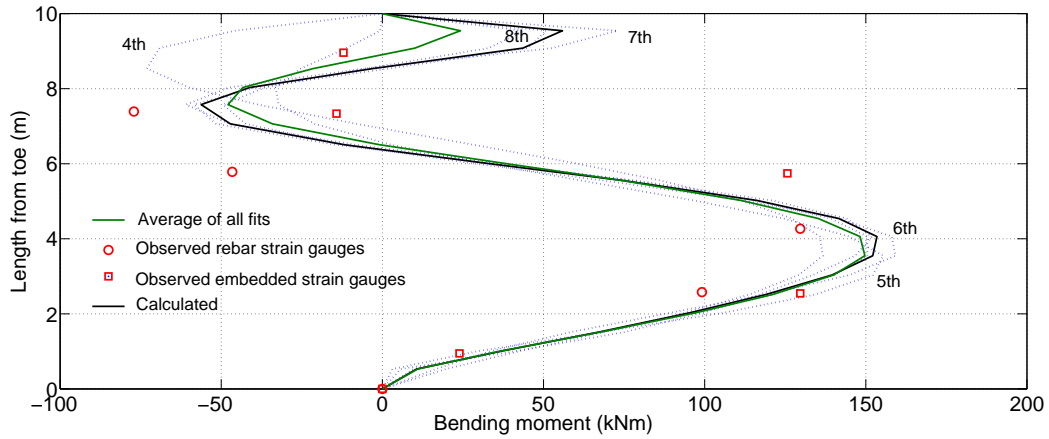
502



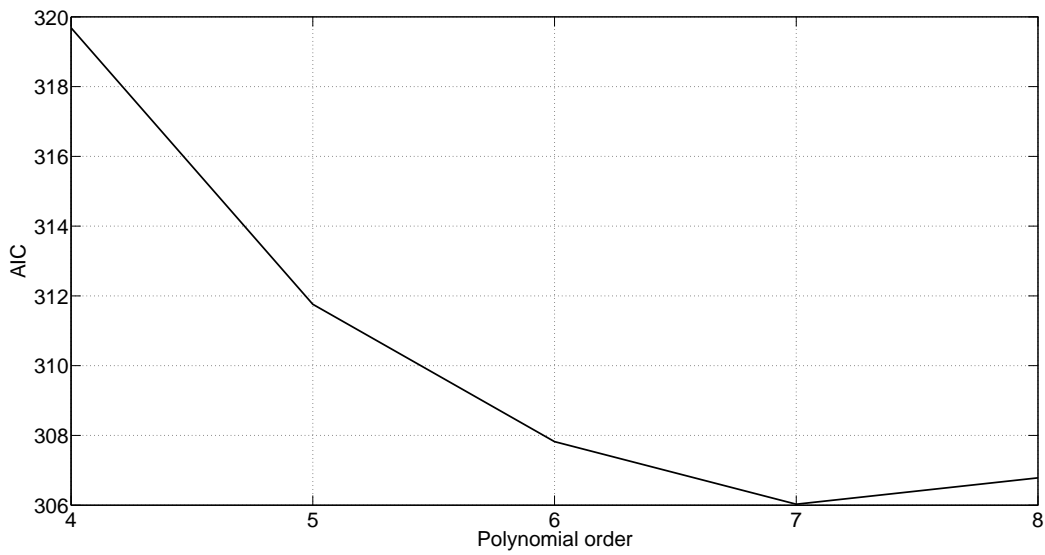
503

504 **Figure A3. Development of method for Liyanapath. & Poulos (2005) (a) Polynomial choice**

505 **(b) AIC**



506



507

508 **Figure A4. Development of method for Smethurst & Powrie (2007) (a) Polynomial choice**

509 **(b) AIC**

510 **NOTATION**

511 a_j distance from toe of the structure to the position where the unit-load

512 is applied

513 A area of cross section of the structure

514 AIC Akaike Information Criterion

| | | |
|-----|--|---|
| 515 | $\mathbf{B}_N, \mathbf{B}_M, \mathbf{B}_V, \mathbf{B}_T$ | matrices which elements are the integrals resulting from the |
| 516 | | application of the method corresponding to the normal, moment, |
| 517 | | shear and torsion internal force distributions respectively |
| 518 | C_0, C_1, C_j, C_n | coefficients of linear equation representing the internal force |
| 519 | | distribution of the real structure |
| 520 | $\mathbf{C}_N, \mathbf{C}_M, \mathbf{C}_V, \mathbf{C}_T$ | arrays of coefficients defining the normal, moment, shear and |
| 521 | | torsion internal force distributions respectively |
| 522 | $d\delta, d\theta, d\rho, d\gamma$ | small displacement of the real structure |
| 523 | E | Young's modulus |
| 524 | G | shear modulus |
| 525 | I | second moment of inertia of cross section |
| 526 | I_p | polar moment of inertia |
| 527 | $f_0(x), f_1(x), f_j(x), f_n(x)$ | functions of linear equation representing the internal force |
| 528 | | distribution of the real structure |
| 529 | f_n | function under evaluation |
| 530 | \hat{f} | estimate of function |
| 531 | h | embedded length in retaining walls |
| 532 | H | retained height in retaining walls |
| 533 | k | number of field measurements of displacements for the real |
| 534 | | structure |
| 535 | L | structure length in retaining walls / piles |
| 536 | n | indication on the number of functions used to approximate the |
| 537 | | internal force distributions |

| | | |
|-----|---|---|
| 538 | $M(\varphi)$ | bending moment of the tunnel |
| 539 | $M_{(j)1}(x)$ | bending moment in the pile / retaining wall caused by the unit-load |
| 540 | | force |
| 541 | $M_{(j)1}(\varphi)$ | bending moment in the tunnel lining caused by the unit-load force |
| 542 | N_1, M_1, V_1 and T_1 | normal stress, bending moments, shear stress and torsion internal |
| 543 | | force distributions of the unit-load structure |
| 544 | $N_{\text{real}}, M_{\text{real}}, V_{\text{real}}$ | |
| 545 | and T_{real} | normal stress, bending moments, shear stress and torsion internal |
| 546 | | force distributions of the real structure |
| 547 | $q(x)$ | external pressure acting on retaining walls / piles |
| 548 | $q(\xi)$ | external pressure acting on tunnel lining |
| 549 | R | radius of tunnel |
| 550 | SSE | Sum of Square of Errors |
| 551 | t | tunnel lining thickness |
| 552 | x | distance from the toe of the retaining wall / pile |
| 553 | u | displacement of real structure in retaining walls / piles |
| 554 | \mathbf{u} | array of field Observed displacements in retaining walls / piles |
| 555 | u_j | displacement of the real structure at the point j where the unit-load |
| 556 | | is applied |
| 557 | u_D | bending component of field measurement displacements in |
| 558 | | retaining walls / piles |

| | | |
|-----|---------------|--|
| 559 | u_D | lateral displacement of pile / retaining wall causing bending |
| 560 | | moments or radial component of distortion displacement at a point |
| 561 | | of the tunnel lining |
| 562 | u_C | uniform convergence displacement |
| 563 | u_O | observed lateral displacement of pile / retaining wall, radial |
| 564 | | displacement of the tunnel lining in the rotated tunnel |
| 565 | u_O^{SL} | radial displacement at the tunnel springline observed |
| 566 | u_{RB} | radial component of rigid body displacement at a point of the tunnel |
| 567 | | lining |
| 568 | u_{RB}^{SL} | radial component of rigid body displacement at the tunnel springline |
| 569 | u_D^{SL} | radial component of distortion displacement at the tunnel springline |
| 570 | u_O^{CR} | radial displacement at the tunnel crown observed |
| 571 | u_{RB}^{CR} | radial component of rigid body displacement at the tunnel crown |
| 572 | u_D^{CR} | radial component of rigid body displacement at the tunnel crown |
| 573 | u_{real} | field Observed displacements in retaining walls / piles |
| 574 | a_s | shear coefficient |
| 575 | b_j | angle measured from the vertical direction clockwise to the point of |
| 576 | | application of the unit-load |
| 577 | d | translation displacement |
| 578 | f | angle measured from the vertical direction at the tunnel crown and |
| 579 | | clockwise |
| 580 | ψ | rigid body rotation |

581 **REFERENCES**

582 Abdoun, T., Dobry, R., O'Rourke, T.D., Goh, S.H. Pile response to lateral spreads:
583 Centrifuge modelling (2003). *Journal of Geotechnical and Geoenvironmental*
584 *Engineering*, **129** (10), 869-878.

585 Anagnostopoulos, C. and Georgiadis, M. (1993). Interaction of Axial and Lateral Pile
586 Responses. *J. Geotechnical Engineering*, **119** (4), 793–798.

587 Akaike, H. (1974). A new look at the statistical model identification. *IEEE Transactions*
588 *on Automatic Control*, **19** (6), 716–723.

589 Brown, D. A., Hidden, S. A., and Zhang, S. (1994). Determination of p-y curves using
590 inclinometer data. *Geotechnical Testing Journal*, **17**(2), 150-158.

591 Brinkgreve, R. B. J., Swolfs, W. M. and Engin, E (2011). *Plaxis Introductory: Student*
592 *Pack and Tutorial Manual 2010*. CRC Press, Inc. Boca Raton, FL, USA.

593 Bozogan, H. (1987). Model selection and Akaike's information criterion (AIC): The
594 general theory and its analytical extensions. *Psychometrika*, **52** (3), 345-370.

595 Carranza-Torres, C., Rysdahl, B., Kasim, M. On the elastic analysis of a circular lined
596 tunnel considering the delayed installation of the support (2013). *International Journal of*
597 *Rock Mechanics and Mining Sciences*, **61**, 57-85.

598 Carranza-Torres, C.,and Diederichs, M. (2009). Mechanical analysis of circular liners
599 with particular reference to composite supports. For example, liners consisting of
600 shotcrete and steel sets. *Tunnelling and Underground Space Technology*, **24**, 506–532.

601 Cheng, C.Y., Dasari, G.R., Chow, Y.K., Leung, C.F. Finite element analysis of tunnel-
602 soil-pile interaction using displacement controlled model (2007). *Tunnelling and*
603 *Underground Space Technology*, **22** (4), 450-466.

604 Curtis, D. J. (1976). Discussion on Muir Wood. The circular tunnel in elastic ground.
605 *Geotechnique*, **26** (1), 213-237.

606 de Sousa Coutinho, A. (2006). Data Reduction of Horizontal Load Full-Scale Tests on
607 Bored Concrete Piles and Pile Groups. *Journal of Geotechnical and Geoenvironmental*
608 *Engineering*, **132** (6), 752-769.

609 Duddeck, H., and Erdmann, J. (1985). On structural design models for tunnels in soft
610 soil. *Tunnelling and Underground Space*, **9** (5-6), 246-259.

611 El Naggar, H., Hinchberger, S. D. and Lo, K.Y. (2008). A closed-form solution for
612 composite tunnel linings in a homogeneous infinite isotropic elastic medium. *Canadian*
613 *Geotechnical Journal*, **45**, 266-287.

614 Fuentes, R. Study of basement design, monitoring and back-analysis to lead to
615 improved design methods. EngD Thesis, University of London, England, 2012.

616 Gaba, A., Simpson, B., Powrie, W., and Beadman D. (2003). Embedded retaining walls:
617 guidance for economic design. Report no 580. CIRIA. London.

618 Gere, J., M. and Timoshenko, S., P. (1987). *Mechanics of materials*, 2nd SI edition. Van
619 Nostrand Reinhold (UK) Co. Ltd, UK.

620 Gonzalez, C. and Sagaseta, C. (2001). Patterns of soil deformations around tunnels.
621 Application to the extension of Madrid Metro. *Computers and Geotechnics*, **28**, 445–
622 468.

623 Hurvich, C. M. and Tsai, C-L. (1991). Bias of the corrected AIC criterion for underfitted
624 regression and time series models, *Biometrika*, **78** (3), 499-509.

625 Inaudi, D., Vurpillot, S., Casanova, N. and Kronenberg, P. (1998). Structural monitoring
626 by curvature analysis using interferometric fibre optic sensors. *Smart Materials and*
627 *Structures*, **7**, 199-208.

628 International Tunnelling Association - ITA (1998). Working group on general approaches
629 to the design of tunnels: Guideliens for the design of tunnels. *Tunnelling and*
630 *Underground Space Technology*, **3**, 237-149.

631 Kim, S. H. Model testing and analysis of interactions between tunnels in clays. PhD
632 thesis, University of Oxford, England, 1996.

633 Liyanapathirana, D. S., Poulos, H. G. (2005). Seismic Lateral Response of Piles in
634 Liquefying Soil. *Journal of Geotechnical and Geoenvironmental Engineering*, **131** (12),
635 1466–1479.

636 Lundquist, E., E., Burke, W., F. (1936). General equations for the stress analysis of
637 rings. Report NACA-TR-509. National Advisory Committee for Aeronautics.
638 <http://naca.central.cranfield.ac.uk/reports/1936/naca-report-509.pdf> (Accessed on
639 11/07/2014)

640 MATLAB R2013b (8.2.0.701). Natick, Massachusetts: The MathWorks Inc., 2013.

641 Mohamad, H., Bennett, P.J., Soga, K., Mair, R.J., Bowers, K. (2010). Behaviour of an
642 old masonry tunnel due to tunnelling-induced ground settlement. *Geotechnique*, **60** (12),
643 927-938.

644 Mohamad, H., Soga, K., Pellew, A., Bennett, P.J. Performance monitoring of a secant-
645 piled wall using distributed fiber optic strain sensing (2011). *Journal of Geotechnical and*
646 *Geoenvironmental Engineering*, **137** (12), 1236-1243.

647 Mohamad, H., Soga, K., Bennett, P.J., Mair, R.J., Lim, C.S. (2012). Monitoring twin
648 tunnel interaction using distributed optical fiber strain measurements. *Journal of*
649 *Geotechnical and Geoenvironmental Engineering*, 138 (8), 957-967.

650 Muir Wood, A. M. (1975). The circular tunnel in elastic ground. *Geotechnique*, **25**(1),
651 115-127.

652 Nip, D. C. N., Ng. C. W. (2005). Back analysis of laterally loaded piles. *The Institution of*
653 *Civil Engineers: Geotechnical Engineering*, **158** (GE2), 63–73.

654 Oreste, P. P. (2003). Analysis of structural interaction in tunnels using the convergence-
655 confinement approach. *Tunnelling and Underground Space Technology*, **18**, 347–363

656 Ou, C.-Y., Liao, J.-T., Lin, H.-D. Performance of diaphragm wall constructed using top-
657 down method (1998). *Journal of Geotechnical and Geoenvironmental Engineering*, **124**
658 (9), 798-808.

659 Panet, M. and Guenot, A. (1982). Analysis of convergence behind the face of a tunnel.
660 *Proceedings Tunnelling 1982 Conference*, 197-204. London

661 Reese, L. C. (1997). Analysis of laterally loaded piles in weak rock. *Journal of*
662 *Geotechnical and Geoenvironmental Engineering*, **123** (11), 1010-1017.

663 Roark, R. (1965). *Formulas for stress and strain*, 4th edition. Mc-Graw-Hill Kogakusha.

664 You, X., Zhang, Z., and Li, Y. (2007). An analytical method of shield tunnel based on
665 force method. *Proceedings of the 33rd ITA-AITES World Tunnel Congress -*
666 *Underground Space - The 4th Dimension of Metropolises*, 791-797.

